Bruno Fradique Lopes Ribeiro

Experimental design and analysis in the neuroscience of decision making: a neuroimaging approach

Dissertação de Mestrado em Engenharia Biomédica, apresentada à Universidade de Coimbra.

Outubro 2016

· U C ·

UNIVERSIDADE DE COIMBRA

Experimental design and analysis in the neuroscience of decision making: a neuroimaging approach

Bruno Fradique Lopes Ribeiro

MASTER'S DEGREE IN BIOMEDICAL ENGINEERING

Physics Department
Faculty of Sciences and Technology of University of Coimbra

Coimbra, 2016

Experimental design and analysis in the neuroscience of decision making: a neuroimaging approach

Author

Bruno F. L. Ribeiro

Supervisor

Miguel de Sá e Sousa de Castelo Branco (M.S., PhD)

Co-Supervisor

Isabel Catarina Castro Duarte (MSc)

Dissertation presented to the Faculty of Sciences and Technology of the University of Coimbra to obtain a Master's degree in Biomedical Engineering

Coimbra, 2016

This project has been developed in collaboration with:

Esta tese é dedicada aos meus pais,

x

Acknowledgements

"No man is an island"

John Donne

Nenhum homem é uma ilha e nenhum projeto se concretiza sozinho. Como tal, quero aqui afirmar o meu reconhecimento a todos quantos me apoiaram nas diversas etapas da concretização deste projeto. Não posso, porém, deixar de fazer algumas referências individuais.

Em primeiro lugar, manifesto o meu profundo agradecimento ao meu orientador e coordenador científico do IBILI Dr. Miguel Castelo-Branco, a oportunidade que me concedeu de realizar a minha dissertação sob a sua orientação. Por todas as ideias e sugestões, por todo o conhecimento e apoio e pela ajuda na resolução dos percalços que inusitadamente foram surgindo.

À Catarina Duarte, que forçosa e imprevisivelmente se viu no papel de minha co-orientadora. Pela dedicação e disponibilidade que sempre demonstrou, por todo o conhecimento que me passou e pela paciência que teve comigo. O seu apoio foi precioso e o contributo determinante para a elaboração desta tese.

À Helena, por tão calorosa e amavelmente me ter aceitado num projeto e num local que eram seus por direito. Por toda a ajuda e pelo empenho e dedicação que demonstrou em todos os momentos, ao longo deste ano.

Um agradecimento especial às instituições acolhedoras do meu projeto - o Instituto Biomédico de Investigação de Luz e Imagem (IBILI) e o Instituto de Ciências Nucleares Aplicadas à Saúde (ICNAS) - por me terem facultado as condições e instalações necessárias para a realização desta dissertação e por terem permitido a minha integração nestes centros de investigação de renome e de elevada qualidade e exigência.

Aos meus amigos, por aguentarem a minha constante loucura. Pela presença e amizade com que sempre me presentearam, não só neste último ano, não só na minha vida académica, mas em todos os instantes. Dirijo um especial agradecimento à Tânia,

pelo apoio, compreensão e dedicação. Por ter acreditado sempre em mim, mesmo naqueles momentos em que este projeto parecia implodir, e por me ter dado a força necessária para continuar.

Aos meus avós, tios e família de Mões, por todo o apoio e carinho com que sempre me envolveram e pela presença e importância que têm na minha vida. Uma palavra de gratidão ao meu tio Mário, pela sabedoria e entusiasmo contagiantes, pela alegria que sempre transmite e, sobretudo, pela sua presença, desde o meu primeiro dia.

Por último, aos meus Pais. Por todo o amor e amizade com que sempre pautaram os meus dias. Pela forma ímpar como veem e vivem cada momento. Pelo sentido de humor único. Pela compreensão e total dedicação. Pela educação e pelos valores que me incutiram. Pelo esforço e sacrifício de cada dia das vossas vidas, que sei serem por mim. Por tudo aquilo que me toleram e suportam. Por me terem dado todas as condições para explorar o meu potencial. Por não terem vacilado quando não o consegui. Pelo carinho, força e compreensão nos piores momentos. Por tudo aquilo que a emoção sente e a razão não consegue exprimir. Por todos os motivos que um simples obrigado parece escamotear. Porque este não é apenas o meu sucesso, mas sim, o nosso sucesso. Obrigado por tudo!

Abstract

Understanding how people make choices under uncertainty is a hot topic in cognitive neuroscience. Decision making is an important feature of brain functioning and embraces several levels, from simple perceptual decisions to goal-oriented behavior under complex emotional and social contexts. Consequently, on a capitalistic modern society, the economic context has gained attention from researchers and a new field has emerged – Neuroeconomics. This novel area embraces several areas, such as neuroscience, psychology and economics.

The present project aims to create and investigate a functional paradigm that allows us to elucidate the brain regions involved in high-level decision making contexts using functional magnetic resonance imaging (fMRI). This thesis generalizes the study of these models to other contexts, namely decision making with impact on other reward variables such as health.

A trust game was designed to analyze the neural correlates of decision making in three different cognitive periods: expectation, investment and feedback. A fundamental question lied on the role of cortical and subcortical regions on decision making processes. How people reacted to reward and punishment and, consequently, updated their judgment was also investigated.

Results here presented revealed the involvement of prefrontal cortex during the processing of expectations, as well as in the feedback period. The reward circuitry also showed important activations in key decision moments, as when participants received high rewards and had that same expectation.

This leads to the additional conclusion that, when the feedback is presented, operant learning processes engage in order to update information so that participants can adjust their choices accordingly. The observed may be helpful in the future to test models of impaired decision making in the context of diseases.

Keywords: fMRI, economy, health, social interactions, decision making, neuroeconomics, reward.

Resumo

Um tema atualmente muito popular no campo das neurociências, prende-se com o modo como as pessoas tomam decisões em contexto de incerteza. A tomada de decisão é uma importante característica funcional do cérebro que abrange diversos níveis: desde simples decisões percetuais a comportamentos orientados por objetivos em diferentes contextos emocionais e sociais. Consequentemente, na sociedade moderna capitalista, o contexto económico tem vindo a ganhar força e os investigadores começaram a virar a sua atenção para este tópico. Nesse sentido, uma nova área despontou – a Neuroeconomia. Este ramo engloba várias especialidades, como neurociências, psicologia e economia.

Este projeto visa a criação e teste de um paradigma funcional que permita elucidar as regiões cerebrais envolvidas em contextos de tomada de decisão de alto nível, usando a técnica de ressonância magnética funcional (fMRI). Esta dissertação generaliza o estudo destes modelos a outros contextos, nomeadamente, tomada de decisão com impacto noutras variáveis, como a saúde.

Um 'jogo de confiança' (trust game) foi concebido para analisar os mecanismos neuronais de tomada de decisão em três períodos distintos: expectativa, investimento e feedback. Outra questão fundamental recaiu no papel das regiões corticais e subcorticais no processo de tomada de decisão. Foi também investigada a diferença da resposta a uma recompensa ou punição, e como a mesma influenciava julgamentos futuros.

Os resultados apresentados revelam envolvimento do córtex pré-frontal, não apenas em momentos de expectativa como seria previsível, mas também no período de feedback. Isto leva a supor que, quando o feedback é apresentado, é ativado todo um processo de aprendizagem operante que reavalia a informação para se ajustarem decisões futuras de acordo com os resultados obtidos na interação. Estes resultados poderão futuramente ajudar a gerar modelos para avaliação dos processos de tomada de decisão em diversos contextos de doença.

Palavras-chave: fMRI, economia, saúde, interação social, tomada de decisão, mecanismos neuronais, neuroeconomia, recompensa.

Symbols & Abbreviations

Symbols

B_0	Magnetic field
ω	Larmor frequency
γ	Gyromagnetic ratio
M_0	Magnetization vector
M_{xy}	Transversal magnetization vector
M_z	Transversal longitudinal vector
X	Design matrix
ϵ	Error vector/matrix
y	Observation vector/matrix
$\hat{Y}$	Fitted values matrix/vector
$\hat{\beta}$	Parameter estimator vector/matrix

Abbreviations

ACC	Anterior cingulate cortex
BOLD	Blood-oxygen-level-dependent
BV	BrainVoyager
BA	Brodmann Area
CSF	Cerebrospinal fluid
EPI	Echo planar imaging
TE	Echo time

FOV	Field of view
FFX	Fixed effects
FID	Free-induction decay
fMRI	Functional magnetic resonance imaging
GLM	General linear model
GP	Globus Pallidus
Hb	Haemoglobin
ISI	Inter stimulus interval
MR	Magnetic resonance
MRI	Magnetic resonance imaging
MCG	Midcingulate gyrus
MTG	Middle temporal gyrus
NAcc	Nucleus accumbens
OFC	Orbitofrontal cortex
OLS	Ordinary least squares
HBO_2	Oxygenated haemoglobin
PCG	Posterior cingulate gyrus
PD	Proton density
RF	Radio frequency
RFX	Random effects
TR	Repetition time
SNR	Signal-to-noise ratio
SSTC	Slice scan time corrections

List of Figures

List of Tables

Contents

Chapter 6

Chapter 1

Introduction

1.1. Motivation and Objectives

Decision making is an important feature of brain functioning, and embraces several levels, from simple perceptual decisions to goal-oriented behavior under complex emotional and social contexts. Understanding how people make choices under uncertainty is a relevant topic in behavioral economics and cognitive neuroscience.

It remains a big challenge to understand the neural mechanisms that drive these decisions. This area has been driven by theoretical modeling, namely economic utility-based models. They are limited to particular contexts of economic decision and not yet generalized to other important contexts of difficult decision. They model utility choice using expected outcome value and risk.

Here we aim to generalize the study of these models to other contexts, namely decision making with impact on other reward variables such as the ones related to self-relevant health related issues. These different contexts are particularly important in

modulating risk magnitude and both interact with individual risk attitude. An important goal is to elucidate the functional recruitment of core and extended neural architectures underlying choice behavior. A trust game adaptation was created in order to evaluate economic and clinical decision making under uncertainty and the neural correlates of the processes involved.

The fundamental aim of this project is to create and test a functional paradigm that allows us to clarify the brain regions involved in high-level decision making contexts, by using a neuroimaging technique – fMRI.

This will, in future, help to generate and test models of impaired decision making in diseases with both impaired/fragmented perception and/or behavioral control such as autism and schizophrenia.

1.2. Dissertation Timeline

These first few lines arise from the need to explain all the tasks proposed in the beginning of this project, as well as the time spent on each step. My Master Thesis project objective was to acquire fMRI data and analyze it in the context of decision making. This project was included within the broader scope of ongoing PhD project that aimed at testing decision making related, using the same paradigm in a clinical population. I helped in the fMRI acquisitions until February (see **Table 1**). In the meantime, I got acquainted with the software that I was going to use for the preprocessing and analysis – BrainVoyager QX v2.6 – and started working on the data that was being collected until approximately mid-march. Some of the control subjects' data acquired along this period became a part of my subject group.

Table 1: Master Thesis Timeline.

Tasks	Sept.	Oct.	Nov.	Dec.	Jan.	Feb.	Mar.	Apr.	May	June	July	Aug.
Literature Review	▓	▓									▓	▓
Patient and Control fMRI acquisitions			▓	▓								
Patient data Preprocessing and analysis					▓	▓						
Project fMRI Acquisitions							▓	▓	▓			
Project Data Preprocessing and analysis									▓	▓	▓	
Writing												▓

1.3. Dissertation Structure

This dissertation is structured in five chapters:

Chapter one is an introduction, where the objectives of this dissertation are stated and the overall structure is defined. A timeline is also given to describe all the work done during the past year.

Chapter two provides a theoretical background for the dissertation theme, where insights on the techniques used are also given. Also, a literature review is presented. I will describe some of the work done in decision making related research and the most notable discoveries regarding brain areas and networks involved in the decision making process.

Chapter three describes the methodology employed, including task procedure and data gathering. Considerations about pre-processing methods are made.

Chapter four presents all the functional results data. Brief considerations regarding the results shown are given.

Chapter five contains the discussion of the previously presented results, the conclusions of the work performed and final considerations, including future work premises.

Chapter 2

Theoretical Background

2.1. Literature review

Our daily routine often puts us in situations where we are confronted with choices and have to make decisions, frequently with unpredictable outcomes and possible repercussions. On that note, understanding how people make decisions under uncertainty is a topic of growing interest within the scientific community.

Decision making is usually defined as the process of choosing the optimal alternative after taking all the other ones into consideration [1][2]. Decisions vary in impact and context, but are often associated with social interactions - social cognition context [3].

These social interactions may be competitive or cooperative [4]. The evolutionary theory predicts mechanisms for deception and manipulation as a "survival of the fittest" struggle, but cooperation is also common due to the society-based culture humans live in [5]. Cooperation and competition involve executive functions and mentalizing

abilities (the capacity to explain and predict the behavior of others by attributing independent mental states to them such as emotions and intentions [6]), both of which play a crucial role during social interactions [4].

Money is said to be the root of all evil but, it's also the base of our capitalist society and a source of many and important social interactions. Consequently, the economic context has been gaining attention from researchers and a new field has emerged: Neuroeconomics [2][7][8]. This field embraces several areas, such as neuroscience, psychology, and economics. It focuses on the cognitive processes underlying economic decision making [2][9], outcome-based decision learning and the individual differences in such processes, using tasks that attempt to be representative of real life [8].

Economic decision making is an example of a context that can be both cooperative and competitive. Cooperation between individuals requires the ability to perceive other's intentions and infer about other's mental states to make cooperative choices [10]. This mentalizing ability is the base of one of the most important traits of decision making: trust. Trust is a social process that helps us to cooperate with others and is often present in human interactions [11]. Trusting is also risky [7], especially given the unpredictability of others' intentions in a social transaction [11].

Recent studies have started to explore the neurobiology of trust [12][13][14] and cooperation [3][15][16][10]. A critical role of trust in nurturing cooperation and solidarity in human society has been emphasized [17][18]. The involvement of the caudate head has been implicated in the computation of information about the fairness of a social partner's decision [12][14]. The orbitofrontal cortex (OFC) and ventral striatum (belonging to the reward circuitry) [19] were associated with high level forms of reward processing, which may come as a result of feelings of trust that reinforce a cooperative act as a recognition that more gains will possibly arise from a mutual cooperation [20][16]. Also, it has been reported evidence that fairness in social interactions is closely related to people's affective linkage [16][14]. Rilling et al, 2002 have also noted a somatosensory association cortex activation and postulated that this was a neural representation of an emotional response to an experience with reciprocated cooperation [15].

The prefrontal cortex, usually implicated in planning complex cognitive behaviors, has also been shown to be active in cooperative actions [10][3]. Decety et al. have revealed that for both cooperation and competitive attitudes, there was an activation of the right superior parietal cortex, superior frontal gyrus and also the anterior insula (usually linked to decision making, consciousness and emotion processing) [3][21].

The nucleus accumbens (NAcc) as part of the reward system, has, as expected, shown activation in reward processing [16][14]. This activation in the NAcc, and plus in the ventral striatum, was also seen in people who expressed revenge feelings towards an unfair trustee [16].

All of these interactions are part of a normal social cognition and adaptive decision making, which has been proven to be related to cingulate and paracingulate cortical activation [19][11]. The paracingulate cortex has also been reported as critical for building a trust relationship by inferring person's intentions to predict subsequent behavior [11]. This brain region can be differently engaged to interact with more primitive (low level) neural systems in maintaining trust in a partnership [11]. Conditional trust has been postulated to selectively activate the ventral tegmental area, a region linked to the evaluation of expected and effective reward, whereas unconditional trust selectively activated the septal area, a region linked to social attachment behavior [11]. Interestingly, there has been research addressing norms such as the ones that imply that trusting strangers is a moral standard in modern society [22].

Many of these brain research studies merely investigated iterated trust processes in which the trustor can learn the trustee's trustworthiness/reputation through some repeated socio-economic transaction games and make trusting/distrusting decisions (knowledge-based trust) [4][23][24][12][11][10][13]. In these kind of fMRI games, each trustor played with the same trustee over multiple trials. This kind of repeated trust games are an adaptation of Berg et al.'s original trust game [25]. There are many variations of the original game, such as: Ultimatum Game [26] and Dictator game [4]. They can be implemented as one-shot trials (one interaction with each trustee) [27] or multiple trials (several interactions with each trustee). In these neuroeconomical games, mathematical decision models are applied to investigate psychological and neuronal correlates underlying social decisions [2].

Furthermore, only a few neuroimaging studies have looked into a single round of trust transaction between two strangers (e.g., [27][28]). Most of the studies were largely focused on how particular trustees reciprocate the trustor's trust rather than how the trustor decides to trust unknown social agents.

Specifically, it was shown that mentalizing (theory of mind), reward and affective processing and cognitive control were important for the trustor to understand the trustee's intentions and to evaluate his or her trustworthiness, which in turn facilitates the trust vs. distrust decision making. Accordingly, brain regions associated with mentalizing (temporo-parietal junction, anterior cingulate cortex (ACC), and posterior cingulate/precuneus) [29][11], reward learning (the head of the caudate nucleus and orbitofrontal cortex), affective processing (insula, amygdala), conflict monitoring and cognitive control (ACC) [30] were activated during the repeated trust game [14][23][12][11][20]. The ACC has been associated with error monitoring, conflict detection and performance monitoring during decision making processes [31][32]. It is possible that some of these brain mechanisms are also involved in generalized trust [33]. Activation of the inferior frontal gyrus is thought to signal subjective risk and supposed to be crucial in the formation of subjective feelings during decision making [19][34].

In a different line of research, other studies focus on the decision making during gambling (win-lose situation) [34]. Many of these studies, addressed the direct influence of prior results to the following decision. They have proven that contrarily to what was thought, people generally tend to be more risk seeking after losing then after winning [35][36]. fMRI results have shown that decisions in winning situation are associated with increased brain activity in the posterior cingulate cortex, while decisions when losing are associated with increased activity in the insula [34]. This reveals a stronger emotional response when losing, which might lead to a riskier behavior. Also, it has been shown that the processes underlying subjective valuation of losses and valuation of winnings were different [7]. Additionally, it has been revealed that the value of a reward relates to factors such as its size, contrarily to a loss [37].

Finally, some research studies have taken the next step and started studying how economic decision making is affected in some diseases (e.g. Parkinson) [38] or context (e.g. age) [31][8]. In both cases, impaired decision making was reported. In the age-related study they were trying to assess whether ageing directly affected decision

making or if, contrarily, it was an indirect effect caused by age-related changes in specific cognitive processes. Their results suggest that impaired decision making is mediated by age-related changes in underlying cognitive capacities [31].

It is, then, important to further study these neuroeconomical trust games, in order to assess the relative role of the involved brain areas in different contexts. This may help us to have a better knowledge on how social behavior and interactions unfold. This knowledge might even be important to understand some behavioral pathologies (sociopathy, psychopathy, autism, etc.). Thus, further implementation of fMRI-based games to other fields (e.g. in the clinical domain) can be very important to the understanding of social interactions in the context of disease.

2.2. Functional Magnetic Resonance imaging (fMRI)

2.2.1. <u>Basic Principles</u>

Magnetic Resonance Imaging (MRI) is a non-invasive imaging technology, often used for disease detection, diagnosis and treatment monitoring. This technique produces three dimensional detailed anatomical images and does not involve the use of ionizing radiation [39]. Over the last decade, it has become the more rigorous, sophisticated and promising clinical diagnostic technique [40].

MRI takes advantage of the intrinsic magnetic properties of the human body, which is primarily constituted by water and fat, to produce detailed images. Fat, water and other macromolecules are constituted by elements, like hydrogen, sodium and carbon, which possess said magnetic properties. Due to its abundance in any biological system and favorable properties, the hydrogen nucleus (single proton) is the most used for clinical imaging purposes [41].

The MRI concept is based upon the interaction of a magnetic field and a nucleus that possesses an overall spin different from zero (e.g. hydrogen nuclei). Spin is a fundamental property of nucleus and it can only admit certain discrete values (multiples of ½).

Under normal circumstances, the nucleus can be considered to spin in the body with their axes randomly aligned, at a constant velocity. Though, when the body is placed in a strong magnetic field, such as inside an MRI scanner, the protons axes line up (see **Figure 1**). This behavior is called Larmor precession (rotation around the direction of the external magnetic field) [42].

(a) No field   **(b)** With field B_0
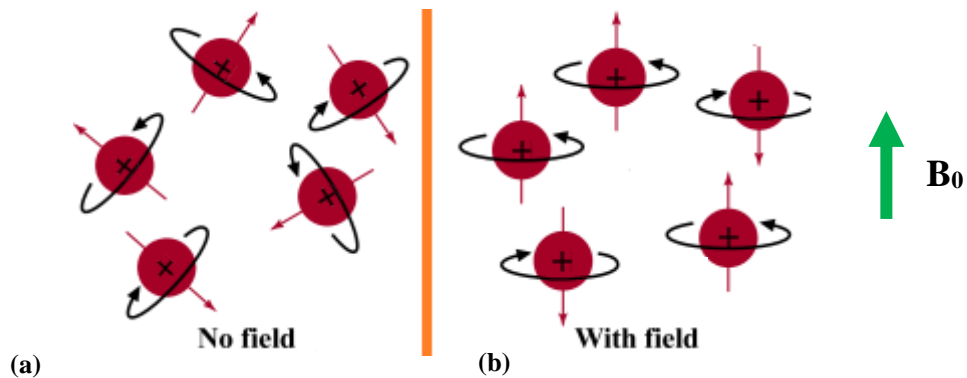
Figure 1. Protons precessing. (a) Protons possess a quantum property of "spin" and can be pictured as spinning around their axes with a random orientation, behaving like small magnetic dipoles. **(b)** When a strong magnetic field, B_0, is applied the protons align their axes with the field in a parallel or antiparallel manner. Adapted from [43].

The frequency of Larmor precession (Larmor or resonance frequency, ω_0) is proportional to the applied magnetic field strength, as defined by the Larmor equation:

$$\omega_0 = \gamma B_0 \qquad \textbf{eq. 2.1}$$

, where γ is the gyromagnetic ratio and B_0 is the strength of the external magnetic field. The gyromagnetic ratio is a nuclei specific constant (**Figure 2**). For hydrogen proton, $\gamma=42.56$ MHz/Tesla.
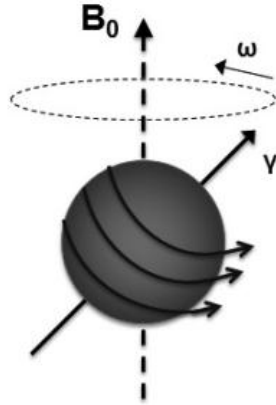
Figure 2. Nuclear Spin precessing in the presence of an external magnetic field B_0 at the Larmor frequency ω [44]**.**

As previously described, in the absence of a magnetic field, the spins will have equal energy and so there will be no preferential alignment between the spins' orientations – null net magnetization vector (M_0) (see **Figure 1a**). However, in the presence of a magnetic field (**Figure 1b**), a parallel orientation will have lower energy and more protons in its configuration than an antiparallel one. This energy difference will be proportional to B_0. Nevertheless, this orientation can be induced. To do so, a radio frequency (RF) pulse with the same frequency as the proton's precession frequency ($ω = ω_0$) has to be applied [45].

The RF pulse (B_1) is applied perpendicularly to B_0 and causes M_0 to tilt away, by an angle α, from B_0 and rotate towards the xy-plane (Mxy) (see **Figure 3**) [44]. The RF pulse intensity and length modulates the extension of the rotation.
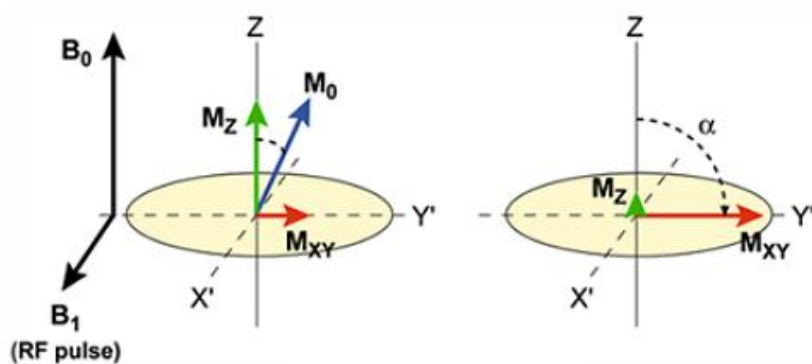
Figure 3. Rotating frame. An RF pulse at the resonance frequency can force the spins to initially precess in phase. As an effect of excitation, the net magnetic field M_0 will rotate

towards the xy-plane. As a result, the longitudinal component Mz decreases while the transverse component Mxy increases. Adapted from [45].

Once the RF signal is removed, the nuclei realign themselves to their original equilibrium positions, i.e., their magnetization moment M_0 becomes parallel with B_0 once again. This process is called relaxation. During relaxation, the nuclei emit their own RF signal, which is measured by a conductive field coil. This signal is called free-induction decay (FID) response signal [42].

There are two types of relaxation that take place simultaneously: longitudinal (spin lattice) and transverse (spin-spin) relaxation.

The longitudinal relaxation is characterized by the T1 relaxation time, which measures the time required for the magnetic moment of the displaced nuclei to recover 63% of its equilibrium after a 90º pulse (**Figure 4**).
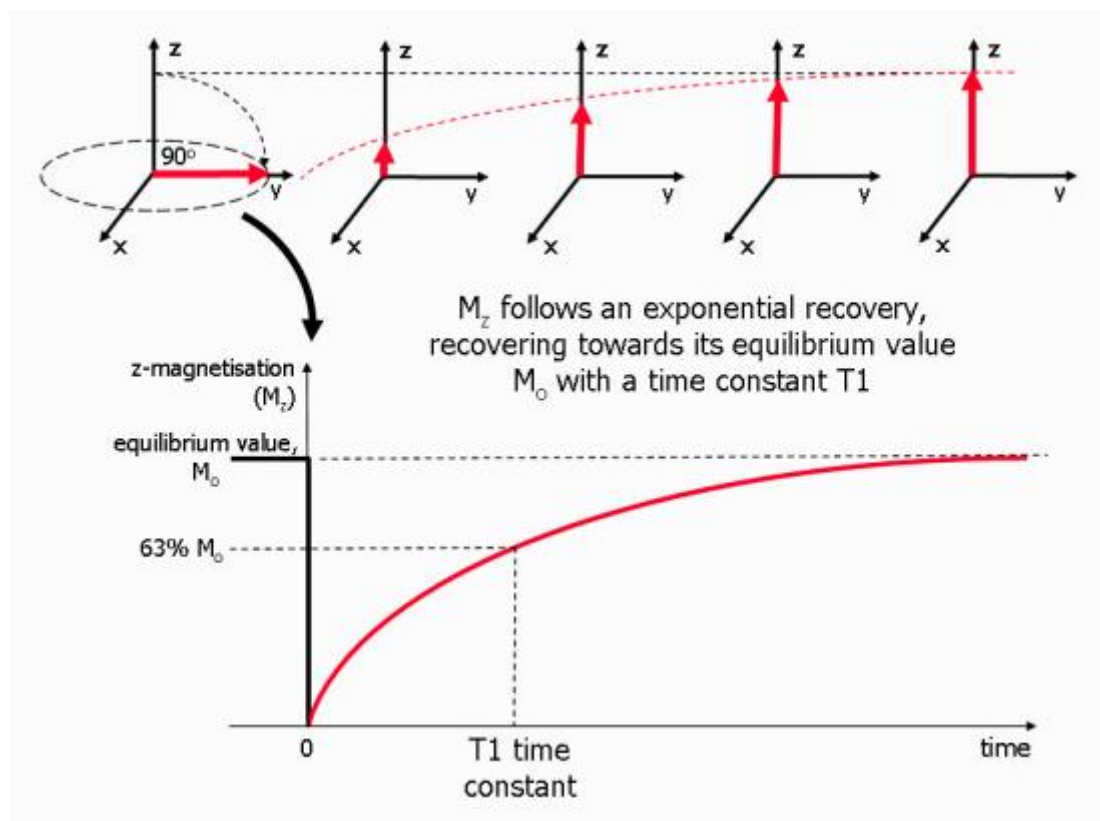
Figure 4. Representation of the T1 relaxation (or recovery) process. Longitudinal relaxation. After a 90º pulse, the system relaxes and magnetization (Mz) will start to return to equilibrium at an exponential rate with a time-constant T1 [46].

T2 is the time constant that characterizes the transverse relaxation and indicates the time required for the FID response signal from a given tissue type to decay to 37% of its original value (**Figure 5**).

However, there is always a certain degree of magnetic field inhomogeneities that lead to a heterogeneous distribution of resonance frequencies. For that reason, the magnetic resonance (MR) signal decreases more rapidly than expected, with a constant decay time T2*.
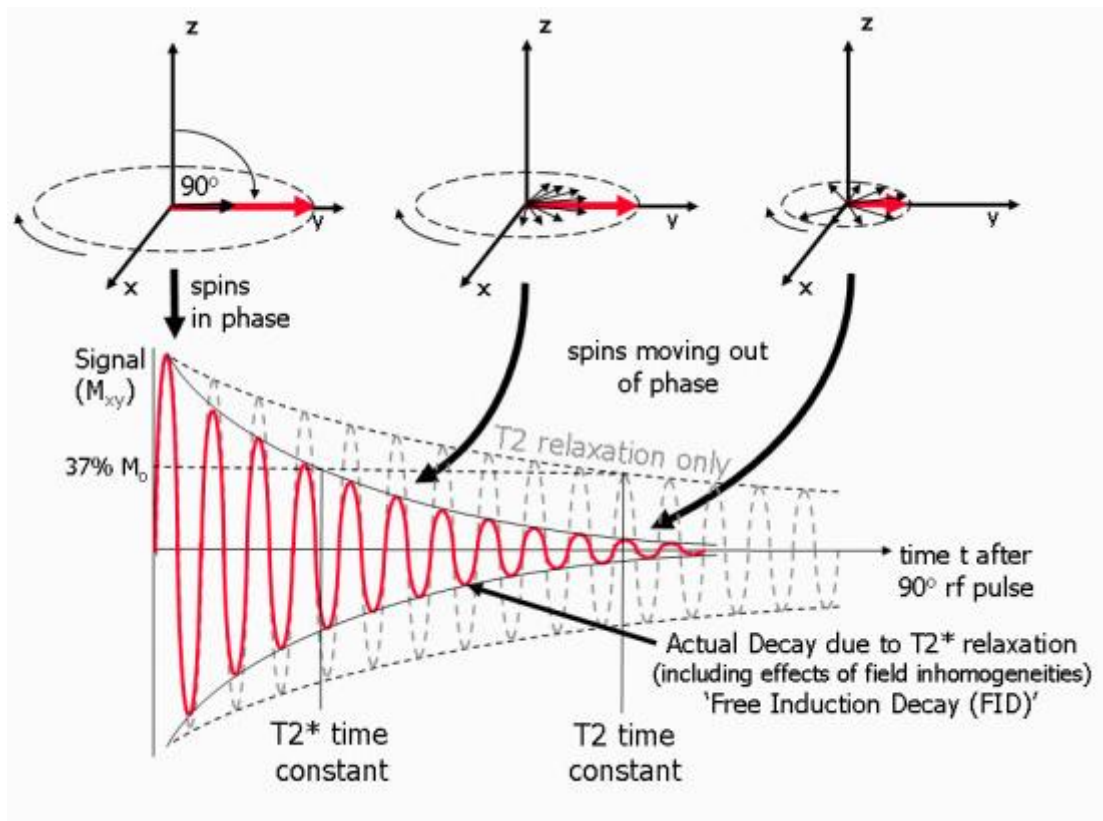
Figure 5. Representation of the T2 relaxation process. Transverse relaxation is the mechanism by which Mxy, the transverse component of the magnetization vector, exponentially decays towards its equilibrium value. The Mxy vector drops to 37% of its original magnitude after a time-constant T2. The real decay occurs at a time constant T2*, which is actually a much smaller value than T2, due to magnetic field inhomogeneities [46].

Different tissues have different T1 and T2 values but T2 always proceeds more rapidly than T1 [42].

However, this relaxation process and the FID signal generated do not give us an image. To produce a 3D image, the FID resonance signal has to be encoded for each

dimension. So, formation of an image involves three steps: slice selection, frequency and phase encoding.

For slice selection, a magnetic field gradient in the z-direction must be applied. Since spins precess at different frequencies along a gradient it is possible to selectively excite a proton. The 2D spatial reconstruction in each axial slice is accomplished using frequency and phase encoding. Both frequency and phase encoding contain spatial information needed for the image reconstruction. This information is stored in the κ-space, where each row corresponds to the frequency information and each column to the phase information. Finally, application of an inverse Fourier Transform is used to transform the encoded image to the spatial domain [47][45][44]. To distinguish different tissues, we need to obtain contrast between them. Contrast is due to differences in the MR signal, which depend on T1, T2, proton density (PD) of the tissues and imaging parameters. Different tissues have different values for T1 and T2. One of the biggest reasons why MRI is so valuable for acquiring images of the brain is because different parts of the brain exhibit different values relative to each other, e.g. the T1 signal for the white matter is stronger than the T1 signal for grey matter, and the grey matter signal, for instance, is stronger than the cerebrospinal fluid (CSF) (see **Figure 6**) [44].
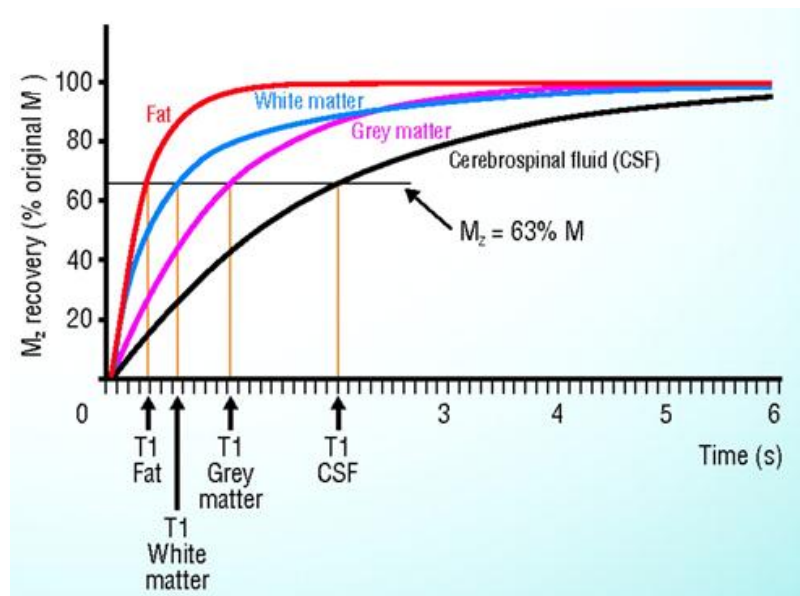
Figure 6. T1 time constant for brain tissue. For any given T1, the white matter signal is stronger than the gray matter, which is stronger than the CSF [48].

14

Contrast is, then, dependent of T1 or T2. It is required to create imaging sequences of RF pulses that display the differences between T1 and T2 time constants. For this, two very important parameters have to be manipulated: repetition time (TR), which is the time between two complete RF pulses, and echo time (TE), which is the time between the RF pulse and the peak of the echo (see **Figure 7**).
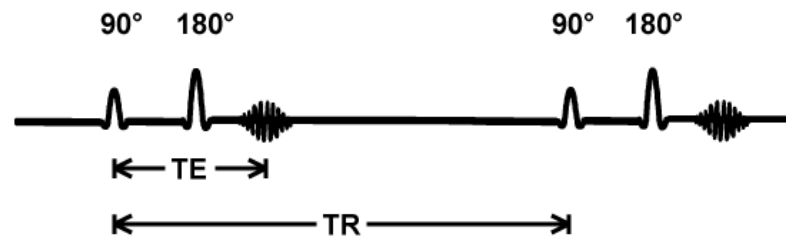
Figure 7. Spin-echo pulse sequence. The spins are initially excited by a 90º pulse, leading them to a diphase in the xy-plane. The system is then exposed to one (or more) 180º pulse that transposes the system, getting the slower spins ahead of the main moment and putting the faster ones behind. Progressively they will all catch up (complete refocusing). This will lead to the formation of an echo. Adapted from [49].

For short values of TR and TE the contrast will be potentiated by the difference in the T1 value of the tissues (T1-weighted sequences or T1 images). On the contrary, using long TR and TE values, contrast will be dependent on T2 differences (T2-weighted sequences or T2 images).

T1 images are often used as anatomical scans, since they have an excellent contrast and clearly display the limits between gray and white matter (**Figure 8a**). They also accentuate fat-rich tissues and soft tissues. T2 images, oppositely, display worse contrast, yet display brain vasculature and abnormal accumulation of fluid (**Figure 8b**) (commonly associated with pathology) better than T1 images.

In conclusion, imaging parameters such as T1 and T2 are very important parameters to take into consideration regarding our needs. The TR and TE parameters can also be manipulated to adjust image contrast for the different tissue types. This is one of the big advantages when comparing MRI with other techniques: a structure that may not be distinctly visible using one of the contrasts, may became exceptionally distinct with one of the other ones.
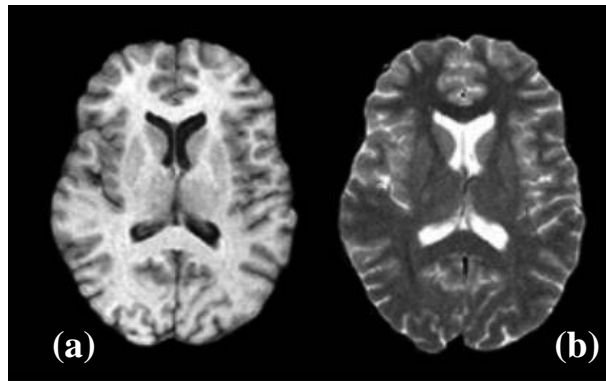
Figure 8. Brain images with two different contrasts. (a) T1-weighted image **(b)** T2-weighted image. Adapted from [44].

2.2.2. <u>BOLD effect</u>

MRI is a powerful imaging technique that allows a good spatial resolution and detail on the various brain structures, something not achieved by any other medical imaging technique.

However, until few years ago, this technique only permitted anatomical information access, not being able to provide data about the function of the organ being studied [50][51]. Nonetheless, the capabilities improvement of MRI equipment led to the extent of this technique to other fields. It made it possible to get relevant information associated with the blood flow, revealing a powerful tool, especially for the study of brain functions[50]. Modern MRI is characterized by being non-invasive, has a spatial resolution of a few millimeters and a temporal resolution that can be less than a millisecond, allowing access to the higher levels of the brain function.

While the idea of a hemodynamic response spatially localized to sites of neural activity dates back to Roy and Sherington (1890), the blood-oxygen-level-dependent (BOLD) method was only proposed in 1990 [50]. The BOLD contrast is a very common method and one of the most used in fMRI, especially in neuroscience. The BOLD contrast relies on the information given by the oxygenation state of the haemoglobin [50] (oxygen is transported by haemoglobin) (see **Figure 9**).

Since the magnetic susceptibility of oxyhaemoglobin and deoxyhaemoglobin is different and T2 MRI parameter is sensitive to inhomogeneities of local fields, it is

16

possible to obtain some information from the different states of haemoglobin. When a given brain area has an increase in neuronal activity, there will be an increase in oxygen through increasing blood flow to that region – hemodynamic response (**Figure 9**).
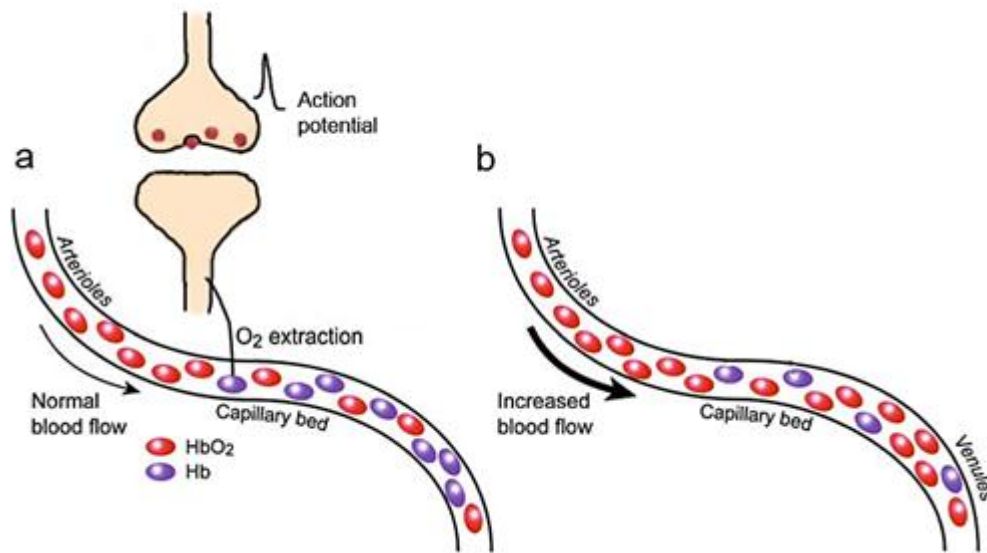
Figure 9. Hemodynamic BOLD response. (a) When an area becomes active there is a fast increase in oxygen consumption, **(b)** which leads to an increase in the blood flow. This results in an increase in deoxygenated haemoglobin (Hb) compared to oxygenated haemoglobin (HbO2). Adapted from [44].

Whether haemoglobin is oxygenated (oxyhaemoglobin) or not (deoxygenated haemoglobin) impacts differently in the MR signal. Oxyhaemoglobin has diamagnetic properties (negative susceptibility to magnetic fields – no permanent net magnetic moment) and therefore does not distort the surrounding magnetic field. On the other hand, deoxyhaemoglobin is paramagnetic (positive susceptibility to magnetic fields due to unpaired electrons) and leads to magnetic field distortions and signal loss [44][31].

The local field inhomogeneities caused by the deoxyhaemoglobin increase the speed of dephasing and the T2* in tissue around the vessels. This was first witnessed in 1990 [50] when it was observed that blood vessels appeared brighter (which may correspond to an increase of T2) when the blood was more oxygenated.

This effect is the basis of the BOLD contrast used in fMRI, where our own blood functions as an endogenous contrast agent. A year later, were observed changes when an animal was breathing an atmosphere low in oxygen. In 1992, the first BOLD contrast studies in humans were performed [52][51].

In spite of this, the BOLD method has a big disadvantage: the differences in the signal which we want to be sensitive are, in fact, small. The percentage of MRI signal that corresponds to the blood is approximately 4% in gray matter and even less in white matter and the differences in blood flow during brain activation stand between 2-5% [53]. So, this method may not be accurate all by himself, hence the need for creating functional paradigms that work as a stimulus to a targeted function [44].

2.3. General Linear Model

The fMRI technique is one of the most widely used methods to study neural correlates. Standard analysis of fMRI data relies on a general linear model (GLM) approach to separate noise from systematic fluctuations of the BOLD signal induced by experimental stimulation [54].

GLM is an extension to a basic linear regression, because it includes more independent variables. It can be used as a univariate, bivariate or multivariate analysis [55]. A univariate analysis (only one variable involved) was the only type of statistical analysis performed here.

An fMRI dataset can be seen as a set of elements (i.e., voxels) with variable dimensions. The goal of a statistical analysis is to determine which voxels have a time-course that correlates with some known pattern of stimulation or experimental manipulation. Firstly, the fMRI data need to be pre-processed in order to correct several potential artifacts that might have appeared during the data acquisition. After that, a GLM analysis may be applied. The aim of this analysis is to determine if, and to what extent, each predictor contributes to the variability observed in the voxel's time-course [54].

GLM is a statistical linear model where the number of observations, represented by the observation vector $y_{N\times1}$ (where N is the number of observations), is related to k unknown parameters, being k the number of predictor variables represented by the vector $\beta_{k\times1}$, through a known design matrix $X_{N\times k}$. $\epsilon_{N\times1}$ is the error vector, that accounts for the unexplained variance of the system.

$$y_{N\times1} = X_{N\times k}\ \beta_{k\times1} + \epsilon_{N\times1} \qquad\qquad \textbf{eq. 2.2}$$

This equation can also be written in its matrix form (**Figure 10**):

$$\begin{bmatrix} y_1 \\ \vdots \\ \vdots \\ \vdots \\ y_n \end{bmatrix} = \begin{bmatrix} 1 & X_{11} & \cdots & \cdots & \cdots & X_{1p} \\ \vdots & \vdots & \vdots & \vdots & \vdots & \vdots \\ \vdots & \vdots & \vdots & \vdots & \vdots & \vdots \\ \vdots & \vdots & \vdots & \vdots & \vdots & \vdots \\ 1 & X_{n1} & \cdots & \cdots & \cdots & X_{np} \end{bmatrix} \begin{bmatrix} b_0 \\ \vdots \\ \vdots \\ b_p \end{bmatrix} + \begin{bmatrix} e_1 \\ \vdots \\ \vdots \\ \vdots \\ e_n \end{bmatrix}$$

Figure 10. GLM matrix [55]**.**

Using the more compact matrix notation, the GLM can be re-expressed, in its simplest formulation**:** y = Xb + ϵ, where y is the column vector of observations, X is the design matrix, b is the column vector of parameters and ϵ is the column vector for of error terms. In the X matrix, the rows correspond to the observations and the columns to the predictors.

So, given a y dataset and an X design matrix, GLM has to discover the adequate beta values (considering e=0). Since generally there are more observations than predictors, this means the design is over-determined, i.e. there's no unique solution. The most common definition is to find the beta values that minimize the sum of squared residuals (error terms) – i.e. the difference between observed and predicted values. This is called the ordinary least squares (OLS) method [56][57].

If X is full column rank, then, the least squares estimates are:

$$\beta = (X^T X)^{-1} X^T Y \qquad\qquad \textbf{eq. 2.3}$$

Satisfying these equation leads to a residual error of $\varepsilon = Y - \hat{Y}$, being $\hat{Y} = X\hat{\beta}$, the projected data.

Minimizing this error value will guarantee, with a certain degree of confidence, that the effects of interest will not be biased by the noise component [58] [59].

2.3.1. <u>Contrasts</u>

After the model parameters have been estimated, specific hypotheses are tested using t or F statistics. In a functional imaging experiment it is often the case that one is interested in many sorts of effects and the possible interactions between them. The more practical approach is to fit larger models and test for specific effects using specific contrasts. Contrasts may be vectors (t-contrasts) or matrices (F-contrasts), which are weighted combinations of the beta values. F-test won't be addressed, since only t-test analyses were performed.

T-contrasts contain a single row (single degree of freedom). As an example, considering a four predictor case, the vector [1 -1 0 0] can be used to find regions where the first condition (c1) is more active than the second (c2). Contrarily, [-1 1 0 0] will show where c2>c1. Conditions can also be compared to an unmodelled baseline (e.g. using the contrast [1 0 0], will show areas more active during the first condition alone).

GLM can refer to a single subject, one group of subjects or various groups of subjects. Although, only multi-subject t-test analyses were presented, single- subject data had to be analyzed and results aggregated, in order to assess commonality and stability of effects within groups of interest [60] [59]. Furthermore, prior to group analysis, for datasets to be comparable across subjects, individual results were molded into a common reference space – Talairach space (Talairach and Tournoux, 1988), in order to align corresponding cerebral structures across subjects with different brain anatomy.

Multi-subject fMRI experiment can also be expressed in a GLM framework with different forms according to the approach taken: fixed, random or even mixed subject analysis.

Random-Effects (RFX) analysis was the approach used in every test performed. This methodology takes into account, not only the within-subject variability, but also makes it possible to make inferences about population in general, contrarily to the Fixed-Effects (FFX) analysis. For a RFX analysis, statistical maps containing estimated effects separately for each subject are required as input. The RFX method is the optimal approach to perform valid population inferences [55].

Chapter 3

Methods

3.1. Participants

Twenty-three healthy individuals were recruited. All subjects were neurologically healthy and did not report a history of mental illness. From this group, two participants were excluded due to software failure that corrupted some of their files; one female did not perform the MRI acquisition due to claustrophobia; and one male's data was not considered for the statistical analysis after the scanning session because was not considered engaged in the task.

The remaining nineteen healthy individuals, 8 males and 11 females, were between 19 and 50 years old (mean age 29.95 ± 9.45 years), with normal or corrected to normal vision. All participants were right-handed and used the joystick with both hands.

All subjects signed the informed consent and the study was approved by the Ethics Committee of the Faculty of Medicine of the University of Coimbra, in accordance with the Declaration of Helsinki.

3.2. Data acquisition

The Magnetic Resonance Imaging (MRI) was performed in a 3T Siemens TrioTim MRI scanner (Siemens, Erlangen, Germany). The scanning session included a high resolution T1-weighted MPRAGE sequence that was measured with TR = 2530 msec, TE = 3.42 msec, TI = 1100 msec, flip angle 7º, single shot slices with voxel size 1 x 1 x 1 mm, FOV (Field of View) 256 mm and a slice thickness of 1 mm, 176 volumes. Functional images were acquired in the same 3T Siemens TrioTim MRI scanner using BOLD contrast echo planar imaging (EPI, TR = 2 sec, TE = 30 msec, 35 slices, voxel size 3 x 3 x 3, in-plane matrix 86 x 86 voxels, 621 volumes) covering the entire brain. These values were identical for both functional acquisitions.

The task was presented to the participant in an LCD monitor (NordicNeuroLab, Bergen, Norway) mounted ~156 cm away from the participants' head. The monitor could be seen through a mirror mounted above the coil. The monitor has a frequency rate of 60 Hz and dimensions of 698.40 x 392.85 mm. The subject could select his response using a MR-compatible joystick (Hybridmojo, San Mateo CA, USA).

3.3. PreProcessing

The data was preprocessed using BrainVoyager (BV) QX v2.6. Preprocessing included the slice scan time corrections (SSTC), temporal filtering and 3D motion correction. Before group analysis, images were transformed into Talairach space and were then spatially smoothed using a 8-mm full-width-half-maximum Gaussian kernel.

After creating the Functional Project on BV, the preprocessing dialog box can be accessed by clicking on Analysis → FMR Data Preprocessing. This will pop-up a menu, where, the operations mentioned before can be selected (see **Figure 11**).

A brief insight on each of these operations will be given hereafter.

All these operations aimed to reduce artifact and noise-related signal components from the raw data.
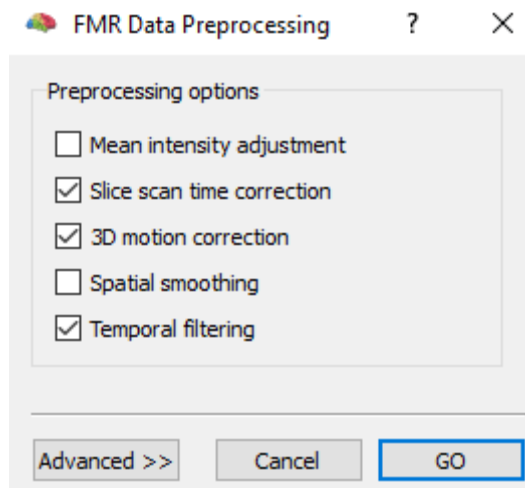
Figure 11. fMRI Data Preprocessing menu.

3.3.1. <u>Slice Scan Time Correction</u>

A sequential 2D imaging technique like single-shot echo planar imaging (EPI) sequence was used as pointed out previously. These single-shot EPI sequences allow for single-slice acquisitions. This means that the whole-brain is not covered at once but, instead, a series of successive 2D slices are sequentially repeated and stacked.

The TR for the whole volume acquisition usually ranges from milliseconds to several seconds, depending on slice thickness. In our study, two seconds were needed to cover whole brain. These time differences between individual slices, cause slice acquisition delays between them (**Figure 12**), since the hemodynamic responses of the individual slices are acquired at different points in time. This may add up to significant temporal shifts over the full 3D volume. These imprecise specifications can lead to statistical biased results, resulting in degraded sensitivity to detect activations.

To compensate for these delays, SSTC realigns slices individually to a reference slice based on its relative timing using an interpolation method – cubic spline interpolation with an ascending interleaved slice scanning order.

Results from Sladky R. et al. in 2011, clearly show a benefit of slice-timing correction for parameter estimation. They indicate that it could significantly improve sensitivity in group statistical analysis [61], proving this to be particularly true for blocked designs with short block length, which was the design used in this project.
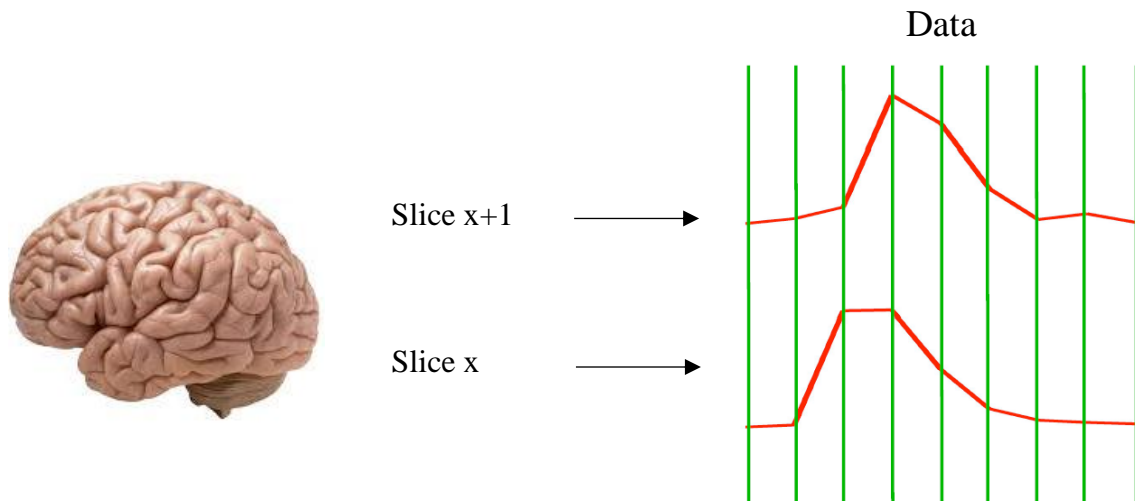
Figure 12. Time differences between consecutive slices without correction [62].

3.3.2. <u>Temporal filtering</u>

Temporal filtering aims to remove or attenuate frequencies within the raw signal, which are not of interest (**Figure 13**).

fMRI data is often disproportionately affected by low-frequency drifts, which are thought to be caused by physiological or physical (scanner-related) noise. These low frequencies reduce substantially the power of statistical data analysis. So, it's generally common to apply a temporal high-pass filter. These high-pass filters help flattening the noise spectrum by removing the low frequency signals without removing signals of interest. This correction helps fulfilling GLM assumptions. Some previous studies, on the efficacy of preprocessing steps, found high pass temporal filtering to significantly enhance one's ability to detect true activations [63][64][65]. Accordingly, a temporal high-pass filter (GLM Fourier) with 2 cycles per point was defined. This means that two sine waves fall within the extent of the data and that every frequency below this value will be removed.
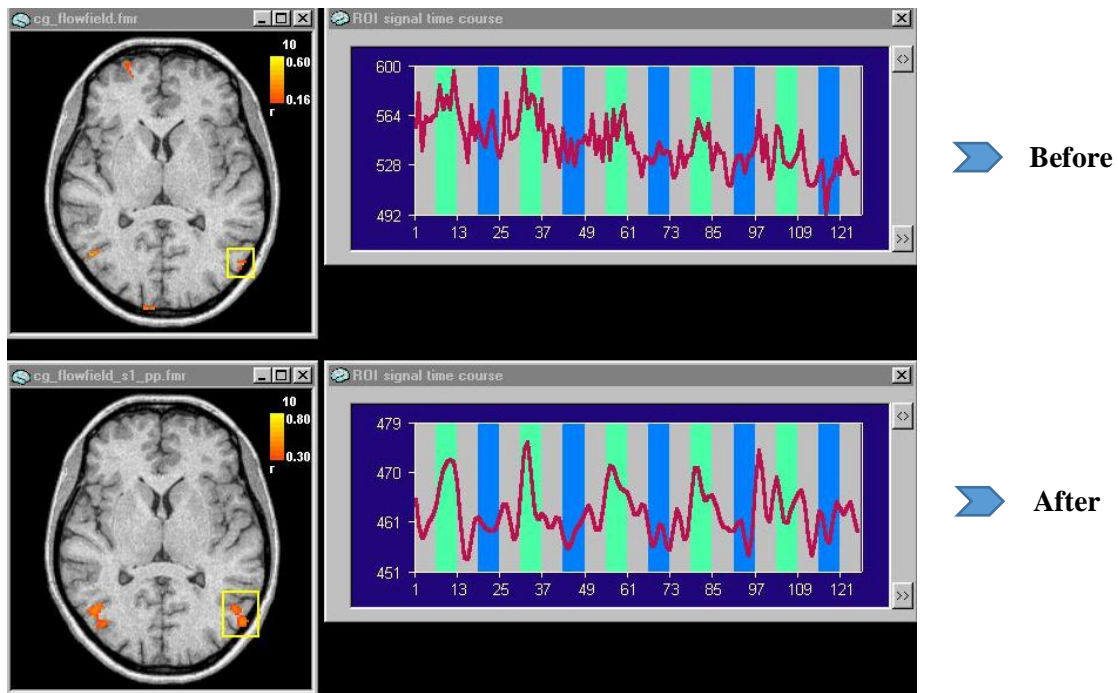
Figure 13. Effect of Temporal Filtering, adapted from [66].

3.3.3. 3D Motion correction

For a proper and reliable analysis of the fMRI data, there's a need for each voxel to correspond to a consistent anatomical point for each point in time [67]. Although there's immobilization equipment around the subject's head, there's always some movement, and displacement of the head reduces the homogeneity of the magnetic field causing artifacts to emerge. These artifacts might present themselves as blurring, geometric distortion, ghosting and/or decreased signal-to-noise ratio (SNR). Their presence reduces the image quality and even scientific relevance [68].

The use of motion correction has been considered a valuable step in preprocessing neuroimaging data with improvements of up to 20% [69].

Motion correction operates by selecting one functional volume of a run as a reference, realigning the other functional volumes to the common reference one. The realignment is applied by rigid body transformations, which can assume that the shape and size of the volumes to be co-registered are the same and that one volume can be spatially matched to another by combination of six body motion parameters (three translation and three rotation parameters). These six degrees of freedom are appropriate only to characterize rigid bodies, since any spatial dislocation of these can be described

by translation and rotation along the x, y and z axes. These parameters are estimated in every iteration in order to get a better alignment with the reference volume. A 3D motion correction with trilinear/sinc interpolation was used. This was the correction option used because, although it runs slower, produces slightly better results than a more simple trilinear interpolation.

3.3.4. <u>Spatial Smoothing</u>

In many fMRI processing pipelines, spatial smoothing is considered a mandatory pre-processing step; it not only allows for random-field approximation based corrections for multiple comparisons, but also for group analysis in standard space [70].

Spatial smoothing is used to reduce high-frequency and increase low-frequency activity components, so as to increase SNR and compensate for functional and anatomical variation across subjects. In this operation, voxel activation values are integrated with neighboring voxel values through convolution with a spatial kernel filter. In other words, data points are averaged with their neighbors.

However, recent studies have indicated that spatial smoothing may systematically bias the localization of reward-related brain activity [71] and further investigation might be needed in this context.

Nonetheless, spatial smoothing is an essential step when preprocessing fMRI data and, in this project, a space domain 3D spatial smoothing with a Gaussian filter of 8.00mm was used.

3.4. Statistical Analyses

Statistical analyses of brain imaging data were performed on individual and group data using the random effects (RFX) General Linear Model (GLM), using BV QX v2.6.

Statistical maps were corrected for multiple comparisons using cluster levels threshold. Cluster correction is based on the assumption that in an fMRI dataset composed of numerous voxels, there is likely to be some correlation in the observed signal between adjacent voxels. That is, one voxel immediately surrounded by several other voxels is not completely independent of its neighbors. The signal in each will be

somewhat similar to the others, and this similarity is roughly related to how close the voxels are to each other. Cluster correction then, uses an algorithm such as Monte Carlo simulations, to determine what number of contiguous voxels at an individual, voxel-wise p-threshold, would be found due to chance alone [55]. The extent of the significant clusters threshold was estimated based on Monte Carlo simulations (1000 iterations).

3.5. Task design and procedure

3.5.1. Paradigm

As previously described, MRI is a diagnostic imaging technique that combines magnetic fields, radiofrequency signals and field gradients to form images of the body. Although it is widely used to probe brain activity and function, currently, BOLD fMRI can only be used to measure relative signal intensity changes, because the signals are not individually quantitative [72]. To measure absolute neuronal activity, an fMRI experiment depends upon paradigms especially designed to quantify relative changes of activity. These paradigms define the tasks executed by the subjects during an fMRI experiment [73].

A block design was the scheme chosen for this study (**Figure 14**). Amongst numerous presentation schemes, this paradigm is one of the most commonly used and the most efficient method for comparing brain responses [72].

This design alternates longer periods of time with a resting state, allowing the contrast of fMRI signals between task blocks (see **Figure 14**). Blocks with longer periods maintain cognitive engagement in a task by presenting continuous stimuli. The sequential alternation between task and rest state throughout the experience ensures that changes, such as subject movements or variations due to scanner sensitivity, will have a comparable impact on the signal response associated to both states [72].

However, maintaining a controlled cognitive state and full concentration during a long period of time, might prove itself to be difficult and this kind of paradigm might not be suitable for each and every experiment.

Simple block paradigm design:

- ▪ Task (stimulus) vs Rest (baseline) or another Task;
- ▪Constant stimulus intensity;
- ▪Constant block lengths;
- ▪Many repetitions.
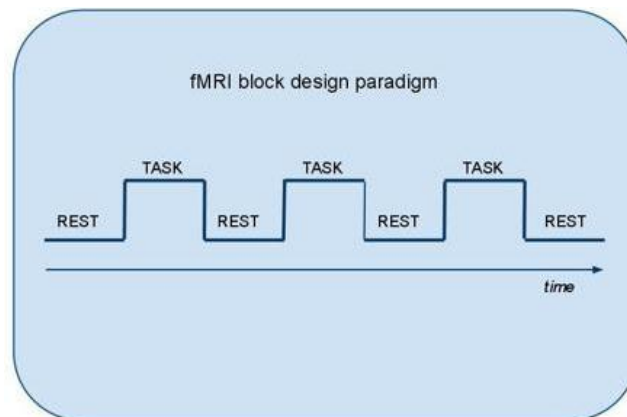
Figure 14. Block design: stimulus of the same condition are presented subsequently. If different conditions are present they should be balanced [74].

3.5.2. <u>Procedure</u>

Participants were positioned in the MRI machine with -a response box (MR-compatible), containing three different buttons. Once inside the scanner, they were then presented with two different tasks (Trust Games): Economic and Clinical game.

The original Trust Game was designed by Berg et al. [25] and it is an experiment used to measure trust in economic decisions. The games presented here are an adaptation of the original Trust Game. Additionally, some adjustments were made to integrate this model into the health context.

Participants were asked to remain as still as possible throughout the entire session. They were familiarized with the task procedure before the fMRI acquisition and told that each response should be given using the three response buttons.

Economic Trust Game

In the Economic game, each subject interacted with four different mediators (trustees). Three of the mediators were unknown humans that matched the subject in gender and the fourth mediator was a computer.

The participant had to negotiate individually with each of the trustees and invest a certain amount of money, knowing that he would receive a certain amount back. The participant was previously informed that the amount of his investment would influence how much he would get. Each human trustee had an inherently different personality and dealt with each investment differently. The computer answered randomly to every investment.

Additionally, before every iteration, participants were asked to guess how much they were expecting to receive from that round's trustee. In every interactive screen was displayed a photo of that round's trustee.

Each iteration started with a fixation cross (8s), followed by the Expected Value screen (8s). This screen had a photo of the trustee and a horizontal slide bar that allowed the participant to choose the amount of money he expected to receive. After the expected value screen, there was an inter-stimulus interval (ISI) with a fixation cross (8s). Then, the Investment screen appeared (8s), asking participants how much they wanted to give to the trustee (0€, 30€ or 50€) with three corresponding buttons. Another ISI was shown (8s) and finally, a Feedback screen appeared (6s), informing the participant how much money he had won that round. Then, there's a final ISI screen (6s) (see **Figure 15** and **Figure 17**). The Expected value and Investment screen would move to the next immediately, without having to wait the 8s maximum, if the participant made a choice within that time.

The economic task consisted of a total of 28 iterations (7 iterations per mediator). The order in which the trustees appeared was pseudo-randomized.

It was pre-determined that the 0's (zero) choice (Null Risk) would always result in a 40€ feedback from every trustee.

The economic task was always the first one performed.
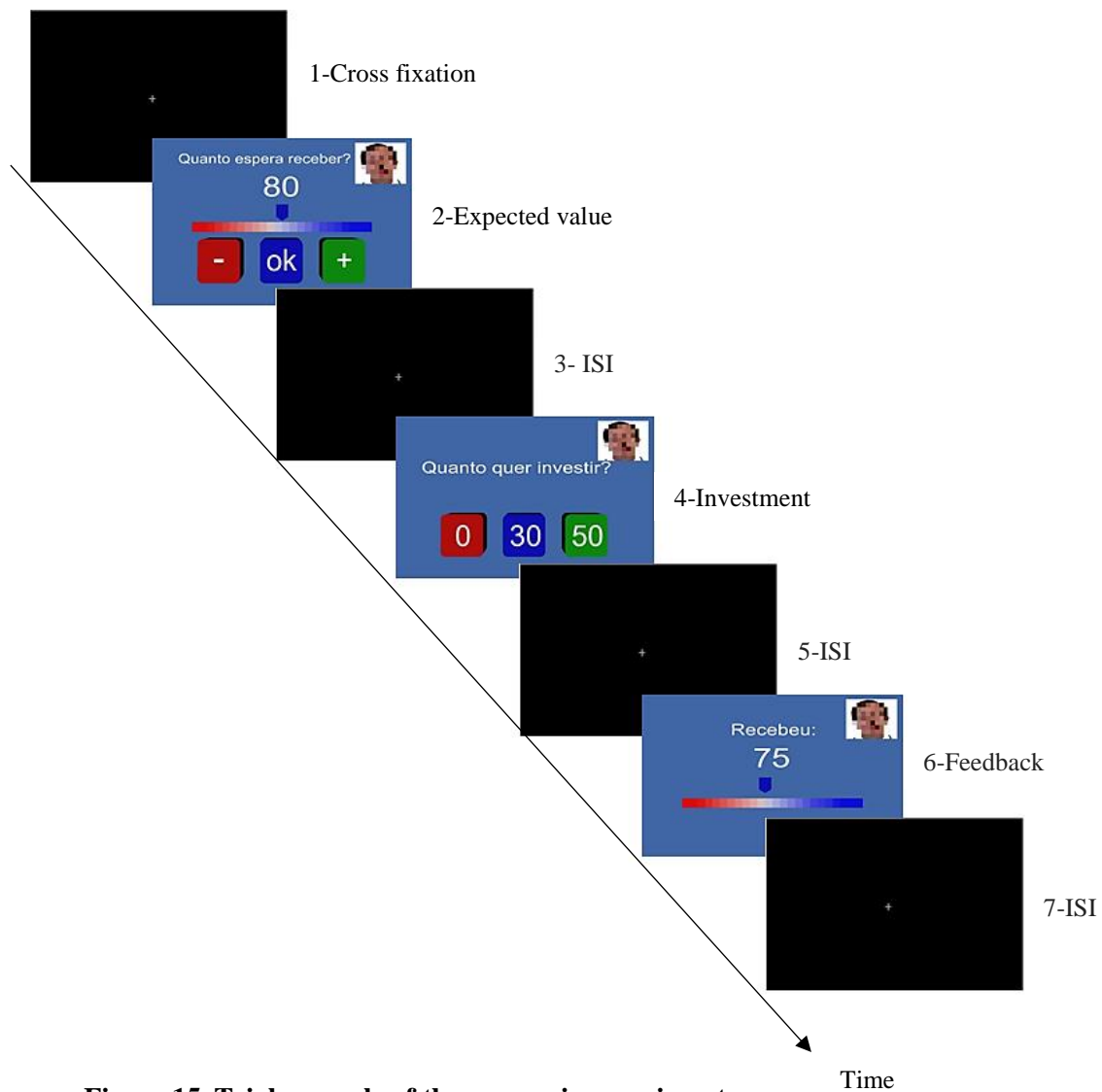
Figure 15. Trial example of the economic experiment.

Clinical Trust Game

The Clinical game was designed similarly to the economic. The aim was to simulate the collaboration of an hypothetical (because we dealt with healthy participants) diabetic patient (who has to continuously shot/inject her/himself for glycaemia levels control) with the clinical professionals. In this task, instead of money, the participant had to decide how many shots/injections she/he was willing to take so that her/his waiting time at a clinical/hospital could eventually reduce. As in the economic task, the participant had first to try to predict how much time he'd have to wait. Then he had to choose how cooperative he wanted to be. Lastly, he was presented to him his waiting time. After the feedback was given, the round ended.

As for the economic game, the clinical game had a total of 28 iterations and the order in which the trustees appeared was randomized.

In this game, however, there were only three trustees. The lottery computer was absent from this task and the participants only had to deal with gender matched human mediators. In their photos, all the trustees were wearing a medical coat and a stethoscope to resemble a Physician.

Each iteration also started with a fixation cross (8s), as in the previous game, followed by the Expected Value screen (8s). This screen had a photo of the trustee and a horizontal slide bar that allowed the participant to choose how much time he thought he'd have to wait, given that trustee. After the expected value screen, there was another ISI (8s). Then, the Investment screen appeared, asking participants how many injections they were willing to take (1, 4 or 6), with three corresponding buttons. Another ISI was shown (8s) and finally, a Feedback screen appeared (6s), informing the participant how much time they would have to wait to be seen by the physician. Then, there was a final ISI screen shown (6s) (see **Figure 16** and **Figure 17**).
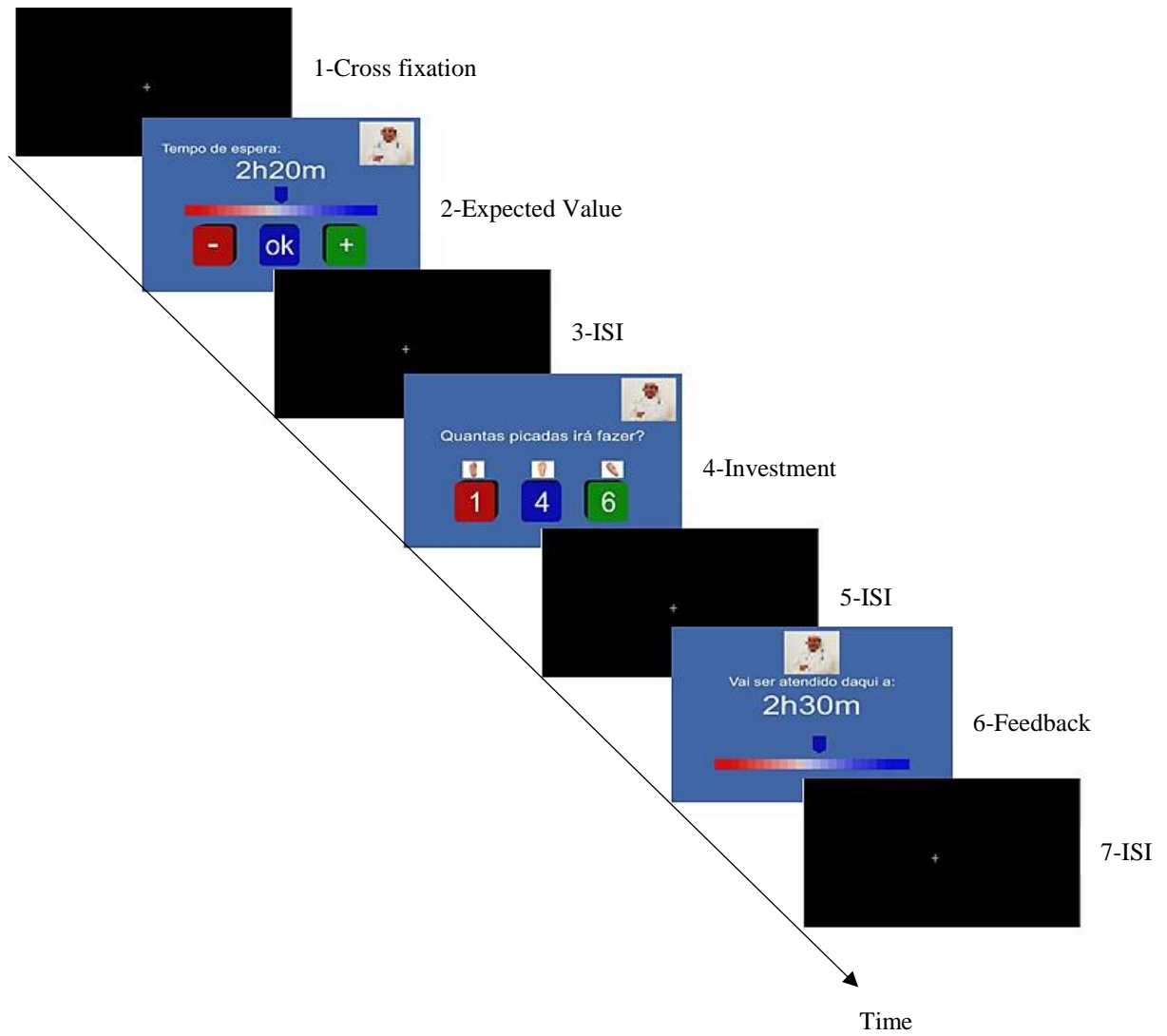
Figure 16. Trial example of the experiment involving health related variables.
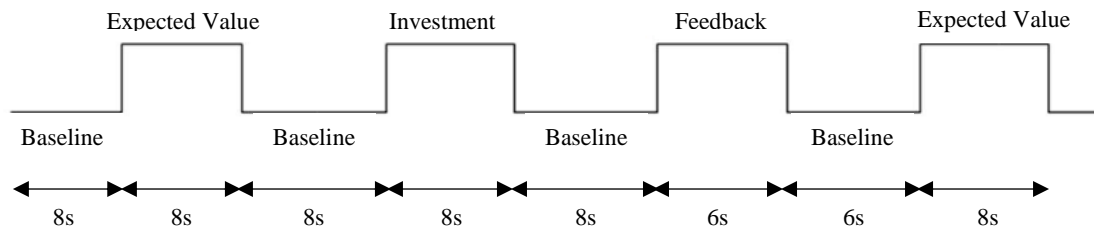
Figure 17. Block design used.

Chapter 4

Results

In this chapter, functional results from the tasks performed by the participants will be presented. This section will be divided in two subsections, each representing a different trust game task: economical and health related. Each of these subsections has five different types of analyses.

4.1. Economic trust - related decision making

RFX contrast analyses were performed for every study. Individual protocols were modified to suit the objective of each analysis. Analyses were performed for every key moment of the task: *expectation*, *investment* and *feedback* periods. Analyses relating feedback with expectations were also executed.

One participant was excluded from three of the economic analyses: Reward contrast, unmatched and matched expectations, due to insufficient number of trials to perform RFX.

4.1.1. <u>Expectation</u>

For this analysis, the mean value of participants' expectations was calculated and set as threshold, thus, dividing the expectations into high and low.

The contrast **High Expectation > Low Expectation** exhibited activations of areas such as the cuneus, lingual gyrus and regions in the right primary somatosensory cortex and left superior parietal lobule (BA7 – Brodmann Area 7). The list of the regions, peak voxel and statistics are described in **Table 2**. This contrast was performed at p<0.01 and using cluster threshold corrections.

Table 2: Results of random effects (RFX) interaction effect, outputs and statistics regarding the contrast High Expectation > Low Expectation.

Region	Peak x	Peak y	Peak z	NrOfVoxels	t	p
R Primary somatosensory cortex: Postcentral gyrus, BA3	35	-23	48	5251	-4.39	0.000350
R Right Cuneus and Lingual gyrus, BA18	14	-65	6	17395	6.37	0.000005
L Superior Parietal Lobule, BA7	-37	-35	45	14875	6.39	0.000005

X, Y and Z represent Talairach coordinates. NrOfVoxels, number of voxels.
Contrasts were performed at **p<0.01** using cluster threshold corrections. R, right; L, left.

4.1.2. <u>Investment</u>

Since investment could only have three possible specific values, division between high and low investments was made considering 0 and 30 as low values and 50 as high. In the investment period, a contrast **High Investment > Low Investment** was performed. When this contrast is verified, active areas appear with an orange color in

the statistical map. When the opposite contrast (Low investment > High Investment) hold true, active areas are shown in blue.

It was found that when participants risked more (high investment), the supra marginal gyrus (BA7 and BA40) was more active (**Figure 18 Figure 20**). On the other hand, when they decided to invest low amounts of money, precentral gyrus, insula and posterior cingulate gyrus were more active than when they invested high amounts. The list of the regions, peak voxels and statistics for this analysis is described in **Table 3**. This contrast was performed at p<0.01 and using cluster threshold.
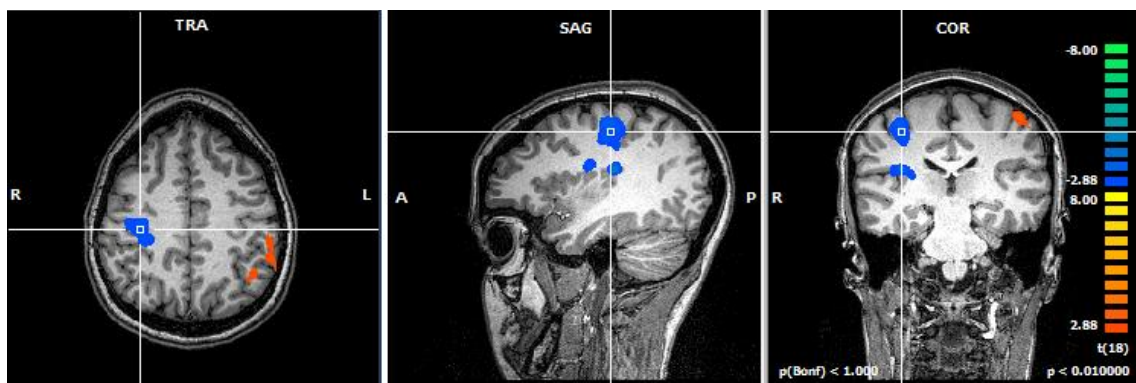
Figure 18. Result regarding the contrast High Investment > Low Investment (Investment period). **R Precentral Gyrus,** BA4. RFX, t(18)>2.88, p<0.01, minimum cluster size of 1269 voxels. The contrast polarity is explained by the fact that different hands report different investment levels.
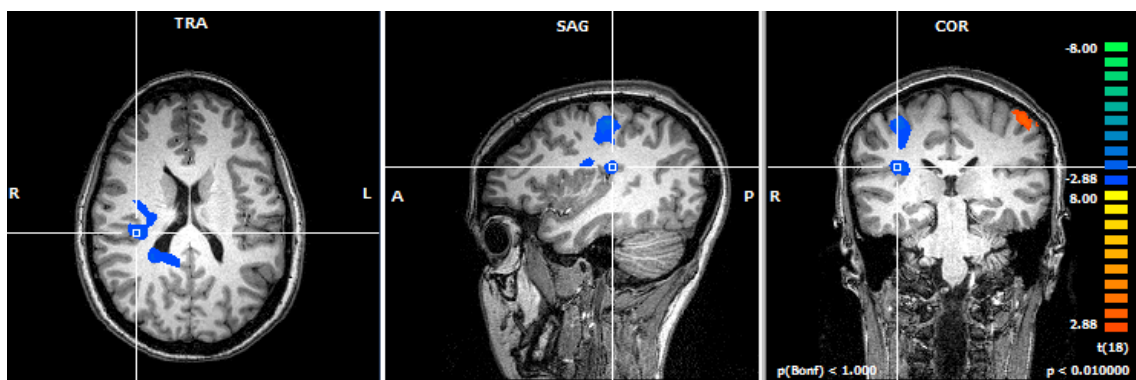
Figure 19. Result regarding the contrast High Investment > Low Investment (Investment period). **R Insula, BA13.** RFX, t(18), p<0.01, minimum cluster size of 1269 voxels.
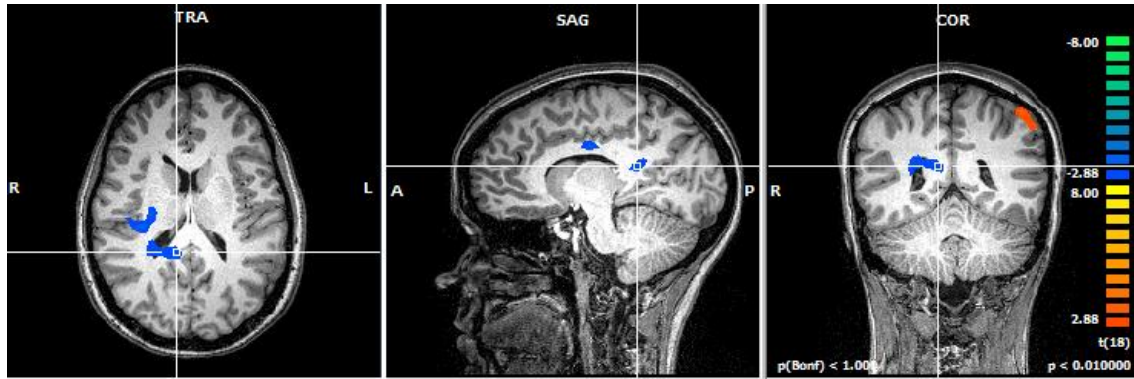
Figure 20. Result regarding the contrast High Investment > Low Investment (Investment period). **R Posterior Cingulate Gyrus, BA29.** RFX, t(18), p<0.01, minimum cluster size of 1269 voxels.

Table 3: Results of random effects (RFX) interaction effect, outputs and statistics regarding the contrast High Investment > Low Investment.

Region	Peak x	Peak y	Peak z	NrOfVoxels	t	p
R Frontal lobe: Precentral gyrus, BA4	**35**	**-20**	**51**	**3302**	**-4.54**	**0.000255**
R Insula, BA13	**35**	**-26**	**21**	**2533**	**-4.50**	**0.000276**
R Posterior Cingulate gyrus, BA29	**11**	**-44**	**18**	**1287**	**-3.95**	**0.000935**
L Inferior Parietal Lobe, BA7 and supramarginal gyrus, BA40	-40	-53	48	4365	4.66	0.000195

X, Y and Z represent Talairach coordinates. NrOfVoxels, number of voxels.
Contrasts were performed at **p<0.01** using cluster threshold corrections. R, right; L, left. Areas in bold are presented in **Figure 18, Figure 19** and **Figure 20**.

4.1.3. <u>Feedback</u>

In a more common trust game adaptation, the feedback is often divided in reward and punishment, e.g., the participants can either receive more money or less money regarding their investment. However, in the game designed for this experience, the trustees were programmed for always giving the participant more money than they invested, meaning that there was never any absolute punishment, only less rewards (a sort of relative punishment). The objective was, then, to assess if there were any differences in brain activation related to the amount of the reward. The threshold for a

high or low amount was defined by calculating the mean value of the trustees' responses.

For the feedback period, a contrast **High Reward > Low Reward** was then performed. When participants received a higher amount (High Reward), areas such as the lingual gyrus, prefrontal cortex (left middle and superior frontal gyrus), left fusiform gyrus and the left middle temporal gyrus were shown to have more activation compared to when participants received lower amounts (Low reward) (**Figure 21-Figure** 23). The regions, peak voxel and statistics for this analysis are described in **Table 4**. This contrast was performed at p<0.01 and using cluster threshold corrections.
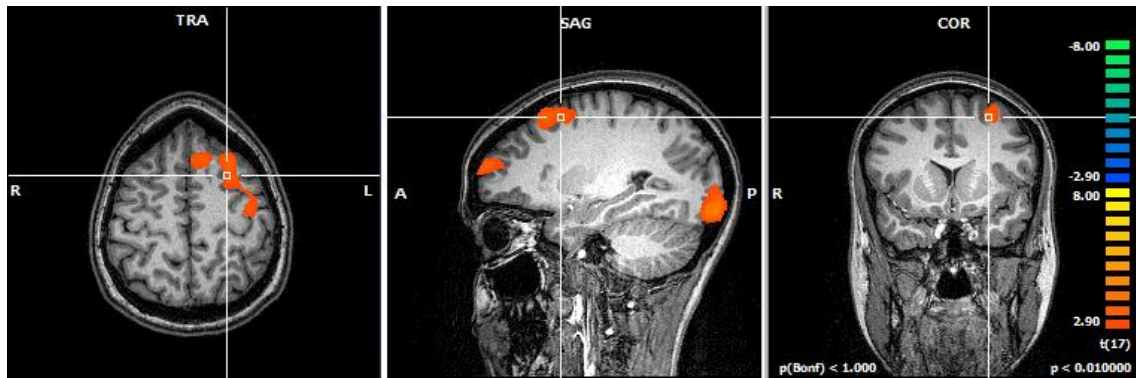
Figure 21. Result regarding the contrast High reward > Low reward (Feedback period). **L Middle frontal gyrus, BA 6.** RFX, t(17), p<0.01, minimum cluster size of 1134 voxels.
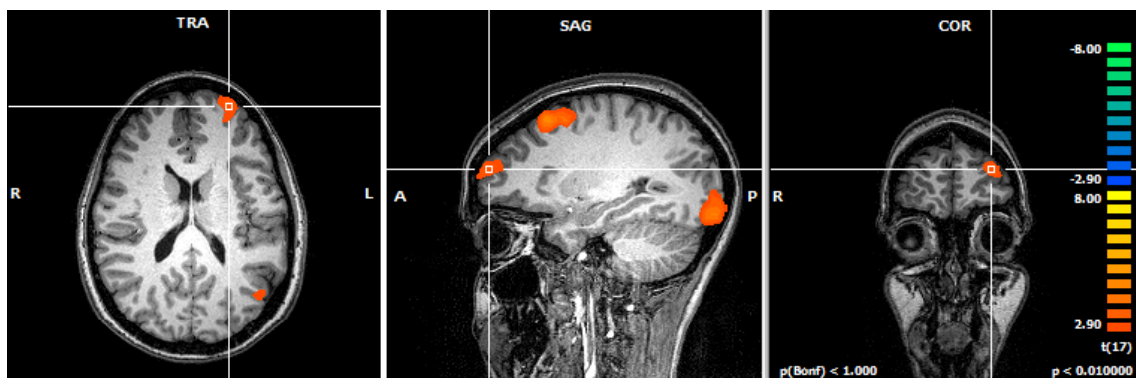
Figure 22. Result regarding the contrast High reward > Low reward (Feedback period). **L Superior frontal gyrus, BA10.** RFX, t(17), p<0.01, minimum cluster size of 1134 voxels.

Figure 23. Result regarding the contrast High reward > Low reward (Feedback period).
L Middle temporal Gyrus, BA19. RFX, t(17), p<0.01, minimum cluster size of 1134 voxels.

Table 4: Results of random effects (RFX) interaction effect, outputs and statistics regarding the contrast High Reward > Low Reward.

Region	Peak x	Peak y	Peak z	NrOfVoxels	t	p
R Prefrontal cortex - Middle Frontal Gyrus, BA6	23	-5	33	3144	4.34	0.000441
R Cerebellum, Culmen BA37 and Fusiform gyrus BA20	38	-56	-21	1572	3.61	0.002171
B Lingual Gyrus, BA17	-7	-95	-6	17428	6.41	0.000006
L Prefrontal cortex – middle frontal gyrus, BA6	**-25**	**19**	**51**	**5015**	**4.95**	**0.000122**
L Prefrontal cortex – superior frontal gyrus, BA10	**-28**	**64**	**15**	**1213**	**4.13**	**0.000699**
L Middle temporal gyrus, BA19	**-46**	**-65**	**12**	**1698**	**4.45**	**0.000350**

X, Y and Z represent Talairach coordinates. NrOfVoxels, number of voxels.
Contrasts were performed at **p<0.01** using cluster threshold corrections. R, right; L, left; B, bilateral. Areas in bold are presented in **Figure 21, Figure 22 and Figure** 23.

4.1.4. <u>Unmatched Expectations</u>

This analysis aimed to consider the feedback period according to the previously formed expectations. Firstly, it was examined the feedback moment when reward did not match the previous expectation (contrast **High Reward in relation to Low Expectations > Low Reward in relation to High Expectations, which can be interpreted as a sort of relative punishment**). When participants received more than

they expected, areas such as parahippoocampal, lingual, precentral (BA4) and fusiform gyri (BA19) were shown to be more active than for when participants received less than they were expecting. The regions, peak voxel and statistics for this analysis are described in **Table 5**. This contrast was performed at p<0.05 and using cluster threshold corrections.

Table 5: Results of random effects (RFX) interaction effect, outputs and statistics regarding the contrast High Reward with Low Expectation > Low Reward with High Expectation.

Region	Peak x	Peak y	Peak z	NrOfVoxels	t	p
R Cerebellum, Culmen and Fusiform gyrus BA20	29	-35	-18	4442	3.93	0.001067
R Lingual gyrus, BA18	-1	-95	12	12998	4.91	0.000132
L Precentral gyrus, BA4	-46	-26	45	4256	3.12	0.006257
L Fusiform gyrus, BA19	-49	-71	-12	5286	3.99	0.000934

X, Y and Z represent Talairach coordinates. NrOfVoxels, number of voxels.
Contrasts were performed at **p<0.05** using cluster threshold corrections. R, right; L, left.

These last contrast conditions were separately compared to the baseline, because they are known not to be symmetrical. Results (see **Table 6**) reveal higher activation of the right middle frontal gyrus, anterior insula (**Figure 24**) and precentral gyrus when the reward was higher than expected (**High Reward with Low Expectation > Baseline**).
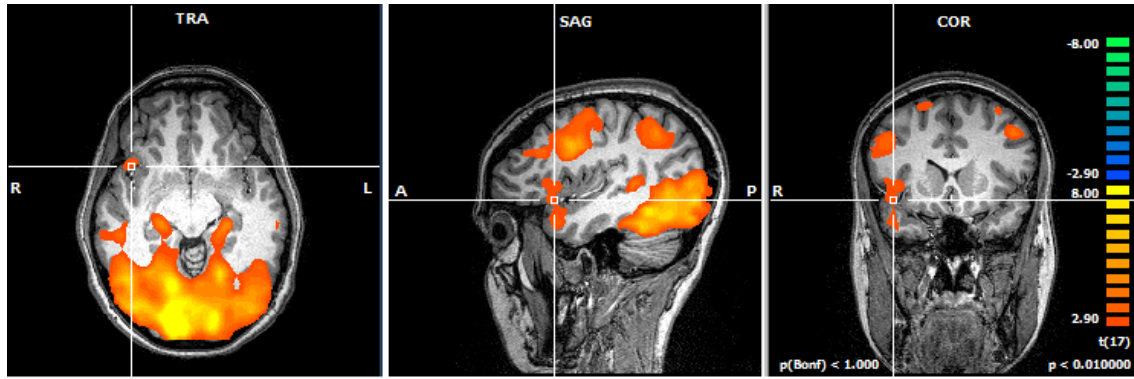
Figure 24. Result regarding the contrast High Reward with Low Expectation > Baseline (Feedback period). **R Anterior Insula, BA13.** RFX, t(17), p<0.01, minimum cluster size of 2997 voxels.

Table 6: Results of random effects (RFX) interaction effect, outputs and statistics regarding the contrast High Reward with Low Expectation compared to baseline.

Region	Peak x	Peak y	Peak z	NrOfVoxels	t	p
B Culmen and Primary visual cortex, BA 17 and 18	14	-80	-12	264248	13.78	0.000001
R Middle Frontal Gyrus, BA6	44	7	33	16617	6.41	0.000006
R Anterior Insula, BA13	**47**	**10**	**-18**	**4078**	**5.96**	**0.000016**
L Middle Frontal Gyrus, BA6	-1	-8	63	8431	5.65	0.000028
L Precentral Gyrus, BA4	-43	-5	42	16929	5.93	0.000016

X, Y and Z represent Talairach coordinates. NrOfVoxels, number of voxels.
Contrasts were performed at **p<0.01** using cluster threshold corrections. R, right; L, left; B, bilateral. Area in bold is presented in **Figure 24**.

On the other hand, when reward was lower than expected (**Low Reward with High Expectation > Baseline**), the same middle frontal and precentral gyrus and insula activations were noted. The superior temporal and the right parahippocampal gyrus were also found active when participants received less than they were expecting. However, bilateral deactivation of the caudate tail was also displayed (**Figure 25**). The regions, peak voxel and statistics for this analysis are described in **Table 7**.
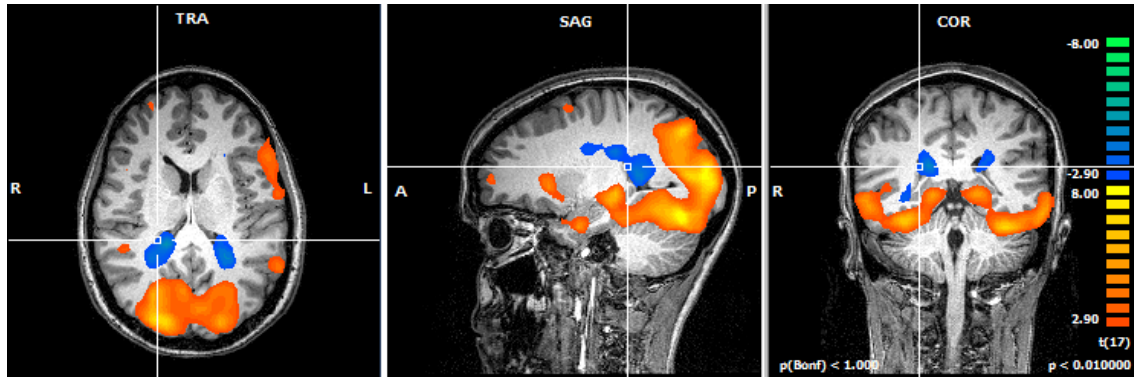
Figure 25. Result regarding the contrast Low Reward with High Expectation compared to baseline (Feedback period). **R Caudate tail.** RFX, t(17), p<0.01, minimum cluster size of 2943 voxels.

Table 7: Results of random effects (RFX) interaction effect, outputs and statistics regarding the contrast Low Reward with High Expectation compared to baseline.

Region	Peak x	Peak y	Peak z	NrOfVoxels	t	p
B Culmen and Primary visual cortex, BA 17 and 18	-7	-92	-18	273233	16.14	0.000001
R Middle Frontal Gyrus, BA6	41	1	33	38590	8.27	0.000001
R Anterior Insula, BA13	26	19	3	5516	5.54	0.000036
R Middle Frontal Gyrus, BA10	32	55	9	2967	5.51	0.000038
R Parahippoocampal Gyrus, BA28	23	-2	-24	3267	5.30	0.000059
R Caudate	**17**	**-38**	**15**	**10375**	**-8.89**	**0.000001**
L Caudate	-25	-47	12	7361	-6.43	0.000006
L Superior Temporal Gyrus, BA38	-49	4	-27	5974	4.67	0.000218
L Precentral Gyrus, BA4	-49	-8	48	26435	5.73	0.000024

X, Y and Z represent Talairach coordinates. NrOfVoxels, number of voxels.

Contrasts were performed at **p<0.01** using cluster threshold corrections. R, right; L, left; B, bilateral. Area in bold is presented in **Figure 25**.

4.1.5. <u>Matched Expectations</u>

Lastly, the neural correlates for when participants received according to their predictions (**Match High Expectations> Match Low Expectations**) were, then, analyzed. When they were expecting to receive a high value and received according to their prediction, middle frontal gyrus (BA6), superior frontal gyrus (BA10), secondary visual cortex and cuneus were shown to be more engaged comparing to when participants received a low amount and were expecting accordingly (**Figure 26** and **Figure 27**). The regions, peak voxel and statistics for this analysis are described in **Table 8**. This contrast was performed at p<0.05 and using cluster threshold corrections.

Figure 26. Result regarding the contrast High Reward with High Expectation > Low Reward with Low Expectation (Feedback period). **R Middle Frontal Gyrus, BA6.** RFX, t(17), p<0.05, minimum cluster size of 3429 voxels. Note also the bilateral activation pattern in parietal cortex.
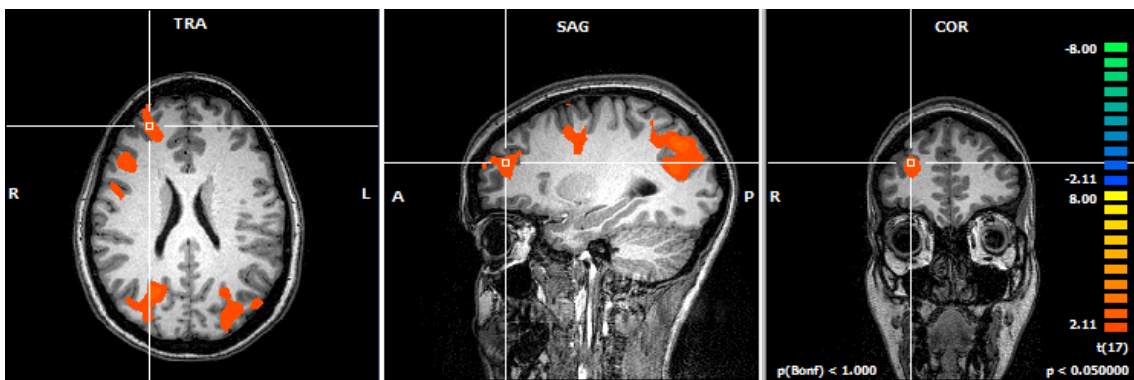
Figure 27. Result regarding the contrast High Reward with High Expectation > Low Reward with Low Expectation (Feedback period). **R Superior Frontal Gyrus, BA10.** RFX, t(17), p<0.05, minimum cluster size of 3429 voxels.

Table 8: Results of random effects (RFX) interaction effect, outputs and statistics regarding the contrast High Reward with High Expectation > Low Reward with Low Expectation.

Region	Peak x	Peak y	Peak z	NrOfVoxels	t	p
R Prefrontal cortex – Middle frontal gyrus, BA6	**50**	**-2**	**39**	**15892**	**4.40**	**0.000394**
R Secondary visual cortex, BA19	26	-71	36	11893	3.85	0.001283
R Prefrontal cortex – Superior frontal gyrus, BA10	**20**	**37**	**18**	**4435**	**3.86**	**0.001248**
L Cuneus, BA17	-4	-98	0	16246	4.30	0.000481

X, Y and Z represent Talairach coordinates. NrOfVoxels, number of voxels.
Contrasts were performed at **p<0.05** using cluster threshold corrections. R, right; L, left. Areas in bold are presented in **Figure 26** and **Figure 27**.

4.2. Health-related decision making

Random Effects (RFX) contrast analyses were performed for every study. Individual protocols were modified to suit the objective of each analysis. Analyses were performed for every key moment of the task: *expectation*, *investment* and *feedback* periods. Analyses relating feedback with respective expectations were also executed. All the 19 participants' data was used for this task analyses.

The analyses performed and the thresholds established similarly to the Economic task. This was accomplished by stipulating a conversion criterion that allowed for values from the health-related task to be converted into economic related values.

4.2.1. Expectation

Results regarding the contrast **High Expectation > Low Expectation** are shown in **Figure 28-Figure** 30. When participants expected to wait less time (High Expectation), regions such as right middle temporal gyrus (BA37), the right globus pallidus, posterior cingulate gyrus (BA26), anterior cingulate gyrus (BA24), secondary visual cortex (BA19) and right postcentral gyrus (BA3-Primary Somatosensory Cortex) were shown to be more active than comparing to when they expected to wait more time

(Low Expectation). When they had lower expectations, the lingual gyrus and the supramarginal and postcentral gyri (BA40) were the regions shown to have greater activations compared to when they had higher expectations. The list of the regions, peak voxel and statistics for this analysis are described in **Table 9.** This contrast was performed at p<0.01 and using cluster threshold corrections.
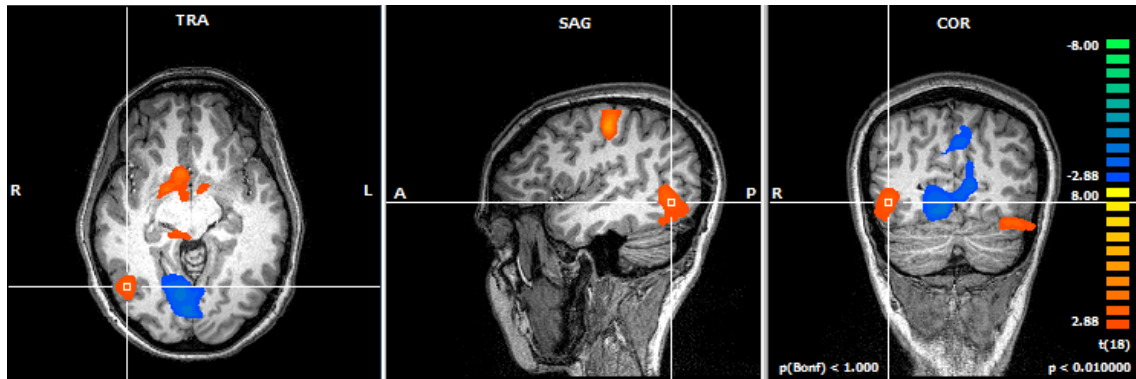
Figure 28. Result regarding the contrast High expectation > Low expectation (Expectation period). **R Middle temporal gyrus, BA37.** RFX, t(18), p<0.01, minimum cluster size of 1431 voxels. Note also the strong activation in **midbrain** and **brainstem** regions.
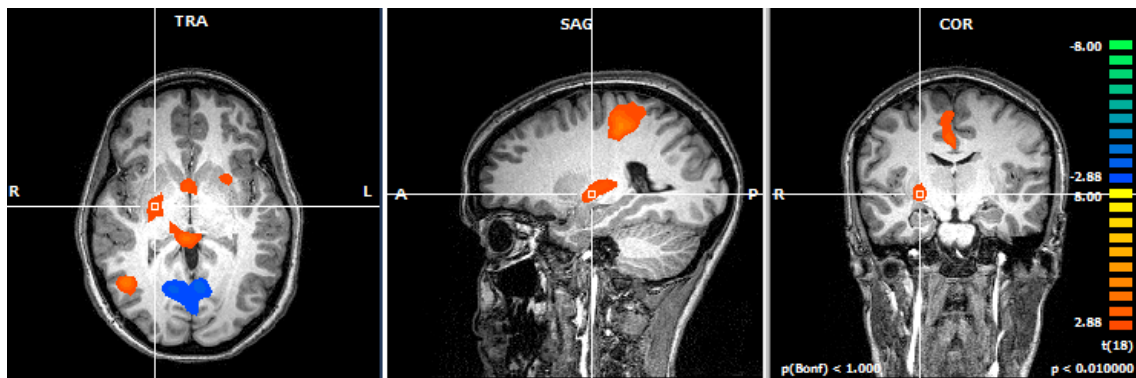
Figure 29. Result regarding the contrast High expectation > Low expectation (Expectation period). **R Globus Pallidus.** RFX, t(18), p<0.01, minimum cluster size of 1431 voxels. Note also the activation of the **caudate** and **putamen.**
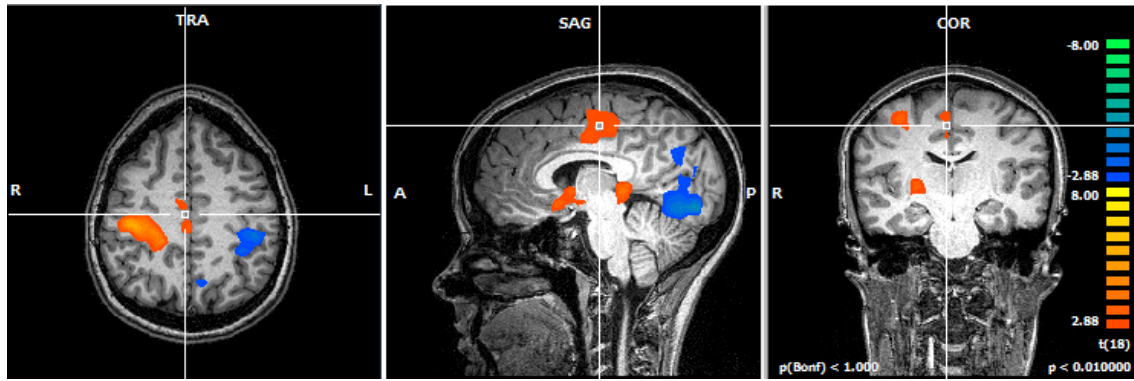
Figure 30. Result regarding the contrast High expectation > Low expectation (Expectation period). **Midcingulate gyrus, BA24.** RFX, t (18), p<0.01, minimum cluster size of 1431 voxels. Note also the activation of posterior **ventromedial/orbitofrontal cortex** and **midbrain regions.**

Table 9: Results of random effects (RFX) interaction effect, outputs and statistics regarding the contrast High Expectation > Low Expectation.

Region	Peak x	Peak y	Peak z	NrOfVoxels	t	p
R Middle temporal gyrus, BA37 and **midbrain, brainstem**	**44**	**-62**	**-3**	**3054**	**4.91**	**0.000113**
R Primary somatosensory cortex, postcentral gyrus, BA3	41	-23	48	11792	6.37	0.000005
R Globus Pallidus	**8**	**13**	**-6**	**6790**	**4.46**	**0.000299**
B Lingual gyrus	8	-74	-12	17821	-5.45	0.000036
B Posterior cingulate gyrus, BA26	5	-32	3	2851	4.38	0.000361
R Midcingulate gyrus, BA24	**5**	**-8**	**39**	**2446**	**3.94**	**0.000956**
B Secondary visual cortex, BA19	-46	-59	-24	8942	4.98	0.000096
L Postcentral and Supramarginal gyrus, BA40	-43	-29	42	3310	-4.39	0.000352

X, Y and Z represent Talairach coordinates. NrOfVoxels, number of voxels.
Contrasts were performed at **p<0.01** using cluster threshold corrections. R, right; L, left; B, bilateral. Areas in bold are presented in **Figure 28, Figure 29** and **Figure 30.**

4.2.2. <u>Investment</u>

In the investment period, a contrast **High Investment > Low Investment** was tested. It was found that when participants decided to invest more (more injections), the

right lingual gyrus and the left precentral gyrus were more active than when they were less cooperative (less injections). The list of the regions, peak voxel and statistics for this analysis is described in **Table 10**. This contrast was performed at p<0.01 and using cluster threshold corrections.
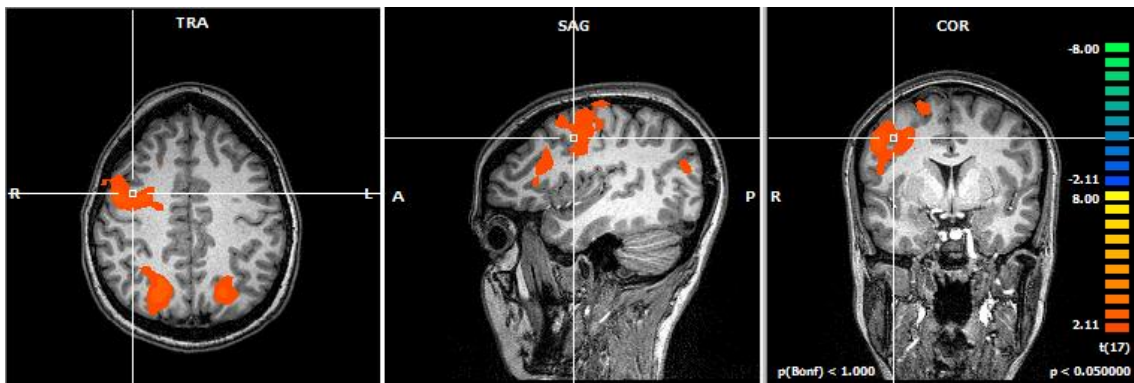
Table 10: Results of random effects (RFX) interaction effect, outputs and statistics regarding the contrast High Investment > Low Investment.

Region	Peak x	Peak y	Peak z	NrOfVoxels	t	p
R Lingual gyrus, BA19	17	-71	-9	5548	4.94	0.000107
L Precentral gyrus, BA4	-34	-29	45	1620	4.11	0.000661

X, Y and Z represent Talairach coordinates. NrOfVoxels, number of voxels.
Contrasts were performed at **p<0.01** using cluster threshold corrections. R, right; L, left.

4.2.3. Feedback

For the feedback period, a contrast **High Reward > Low Reward** was performed. When participants were told they would have to wait a small amount of time (High Reward), an activation of the prefrontal cortex – left superior frontal gyrus (BA10) – was detected compared to when participants had to wait more time (Low reward) (**Figure 31**). Details are described in **Table 11**. This contrast was performed at p<0.06 and using cluster threshold corrections.
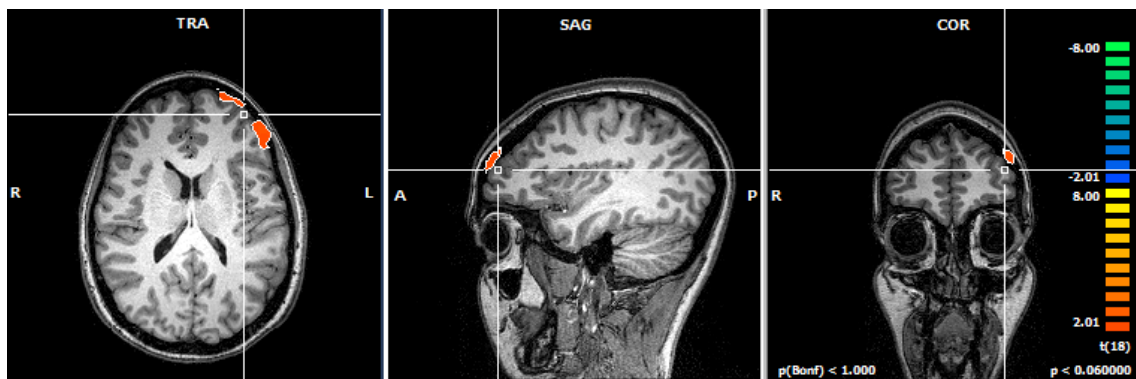
Figure 31. Result regarding the contrast High reward > Low reward (Feedback period). **L Superior frontal gyrus, BA10, in frontal polar cortex.** RFX, t(18), p<0.06, minimum cluster size of 3267 voxels.

Table 11: Results of random effects (RFX) interaction effect, outputs and statistics regarding the contrast High Reward > Low Reward.

Region	Peak x	Peak y	Peak z	NrOfVoxels	t	p
L Superior frontal gyrus, BA10	**-13**	**64**	**24**	**4064**	**3.70**	**0.001641**

X, Y and Z represent Talairach coordinates. NrOfVoxels, number of voxels.
Contrast was performed at **p<0.06** using cluster threshold corrections. L, left. Area in bold is presented in **Figure 31**.

4.2.4. <u>Unmatched Expectations</u>

As in the economical task, after the main block related contrasts were analyzed, the feedback period was evaluated according to the previously formed expectations. The relation between reward and expectation considered for this analysis was unmatched (contrast **High Reward in relation to Low Expectations > Low Reward in relation to High Expectations**). When participants waited more than they expected the postcentral gyrus was shown a deactivation compared to when participants received more than they were expecting. The region, peak voxel and statistics for this analysis are described in **Table 12**. This contrast was performed at p<0.05 and using cluster threshold corrections.

Table 12: Results of random effects (RFX) interaction effect, outputs and statistics regarding the contrast High Reward with Low Expectation > Low Reward with High Expectation.

Region	Peak x	Peak y	Peak z	NrOfVoxels	t	P
L Postcentral gyrus	-31	-32	45	6723	-3.75	0.001480

X, Y and Z represent Talairach coordinates. NrOfVoxels, number of voxels.
Contrast was performed at **p<0.05** using cluster threshold corrections. L, left.

The unmatched expectations contrasts were then performed separately comparing to the baseline, because they assymetrically reflect reward vs punishment. Superior and inferior frontal gyri, as well as the precentral gyrus, were found to be active when they

had to wait less time than they expected comparing to baseline (see **Figure 32** and **Table 13**).
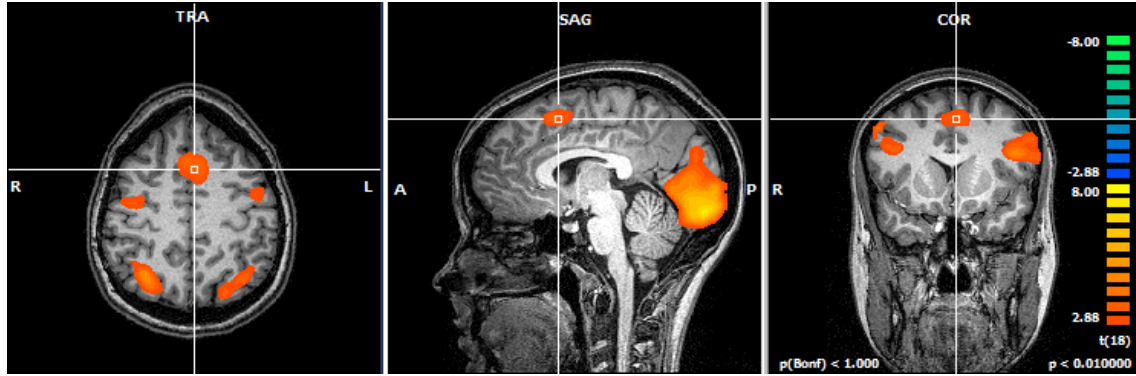
Figure 32. Result regarding the contrast High Reward with Low Expectation compared to Baseline (Feedback period). **L Superior frontal gyrus, BA6.** RFX, t(18), p<0.01, minimum cluster size of 2619 voxels.

Table 13: Results of random effects (RFX) interaction effect, outputs and statistics regarding the contrast High Reward with Low Expectation compared to Baseline.

Region	Peak x	Peak y	Peak z	NrOfVoxels	t	p
R Precentral gyrus, BA4	41	1	33	11012	6.86	0.000002
B Lingual Gyrus and Inferior Occipital Gyrus, BA17 and 18	11	-92	0	175302	10.56	0.000001
B **Superior Frontal Gyrus**, BA6	5	16	48	2895	5.00	0.000092
L Inferior Frontal Gyrus, BA9	-37	-2	36	12404	6.23	0.000007

X, Y and Z represent Talairach coordinates. NrOfVoxels, number of voxels.
Contrasts were performed at **p<0.01** using cluster threshold corrections. R, right; L, left; B, bilateral. Area in bold is presented in **Figure 32**.

Punishment results (**Low Reward with High Expectations > Baseline**) were similar to great reward results (waiting less time) (see

Table 14), as activations of the inferior and middle frontal gyri were also observed. Caudate deactivation displayed, like when the same contrast was applied to the economic-related task (**Figure 33**).
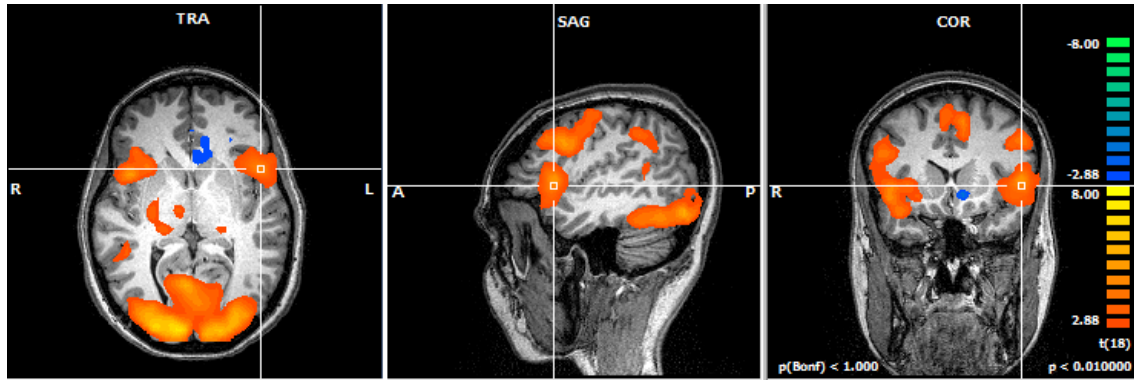
Figure 33. Result regarding the contrast Low Reward with High Expectation compared to Baseline (Feedback period). **L Inferior frontal gyrus, BA9 and Insula, BA13.** RFX, t(18), p<0.01, minimum cluster size of 2754 voxels.

Table 14: Results of random effects (RFX) interaction effect, outputs and statistics regarding the contrast Low Reward with High Expectation compared to Baseline.

Region	Peak x	Peak y	Peak z	NrOfVoxels	t	p
B Lingual Gyrus and Cuneus, BA 17 and 18	-7	-92	-12	226095	9.38	0.000001
L Middle Frontal Gyrus, BA9	2	-8	60	31567	5.97	0.000012
L Caudate	-7	16	0	3234	-4.94	0.000107
L Inferior Frontal Gyrus, BA9 and **Insula**, BA13	-46	13	9	9621	9.60	0.000001

X, Y and Z represent Talairach coordinates. NrOfVoxels, number of voxels.
Contrasts were performed at **p<0.01** using cluster threshold corrections. L, left; B, bilateral. Area in bold is presented in **Figure 33**.

4.2.5. Matched Expectations

Lastly, a matched expectations analysis was conducted (**Match High Expectations > Match Low Expectations**). When participants were expecting to have to wait less time and indeed the results were according to their prediction, the gyrus rectus (BA11), the putamen and the left middle frontal gyrus were shown to be more engaged comparing to when participants received the feedback that they would have to wait more time and were expecting accordingly (**Figure 34** and **Figure 35**). Contrarily, the right caudate body and tail showed increased deactivation in the same scenario. The

regions, peak voxel and statistics for this analysis are described in **Table 15.** This contrast was performed at p<0.05 and using cluster threshold corrections.

Figure 34. Result regarding the contrast High Reward with High Expectation > Low Reward with Low Expectation (Feedback period). **Gyrus Rectus, Orbitofrontal cortex BA11.** RFX, t(18), p<0.05, minimum cluster size of 2916 voxels.
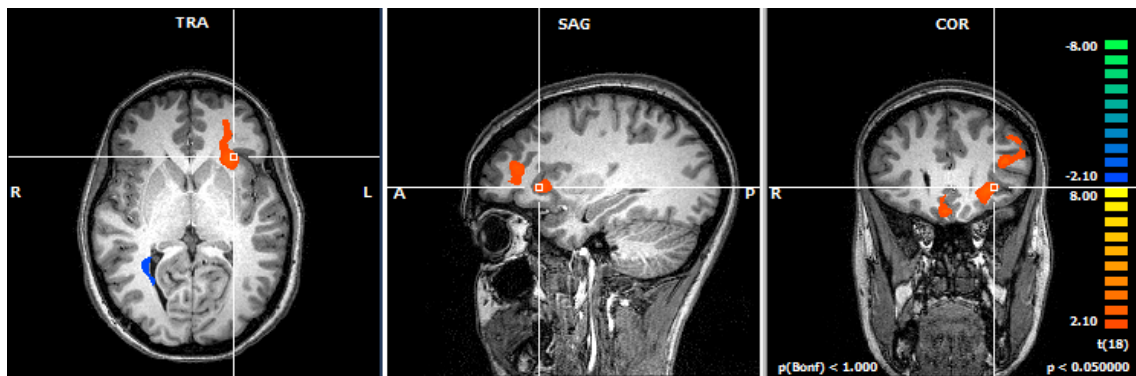
Figure 35. Result regarding the contrast High Reward with High Expectation > Low Reward with Low Expectation (Feedback period). **Anterior Insula/Claustrum.** RFX, t(18), p<0.05, minimum cluster size of 2916 voxels. Note the activation in the orbitofrontal cortex and other regions of anterior frontal cortex.

Table 15: Results of random effects (RFX) interaction effect, outputs and statistics regarding the contrast High Reward with High Expectation > Low Reward with Low Expectation.

Region	Peak x	Peak y	Peak z	NrOfVoxels	t	p
R Caudate Tail and Body	23	-26	24	3032	-2.90	0.009457
B Gyrus Rectus, Orbitofrontal cortex BA11	**8**	**31**	**-15**	**6177**	**3.79**	**0.001330**
L Anterior Insula; Claustrum	**-22**	**22**	**3**	**4318**	**4.82**	**0.000137**
L Middle Frontal Gyrus	-37	19	24	4565	3.56	0.002213

X, Y and Z represent Talairach coordinates. NrOfVoxels, number of voxels.
Contrasts were performed at **p<0.05** using cluster threshold corrections. R, right; L, left; B, bilateral. Areas in bold are presented in **Figure 34 and Figure** 35.

Chapter 5

Discussion and Conclusion

5.1 Discussion

As stated, the major aim of this project was to create and test a functional paradigm that would allow us to understand which brain areas become active in key decision making moments, related to self-relevant variables beyond monetary value. This, will not only let us to know more about neural architecture and mechanisms of decision making in the brain, but it will also help to generate models of impaired decision making in the clinical setting.

Since decision making focus, not only, in weighting the costs of risky choices, but also in the possibility of reward outcomes [75], neural regions associated with risk attitudes, reward processing and trustworthiness judgments were taken into account. The separation between the different cognitive phases of the experience (expectation, investment and feedback periods) made it possible to isolate them and to analyze the underlying neural correlates of each one of them.

Summarily, expectation phase showed activation of perceptive, emotional and learning areas, such as globus pallidus (GP) and midcingulate gyrus (MCG). It was postulated that this was due to the updating of information regarding each trustee that led to the consequent prediction. Reward-seeking associated areas, like the PCG and insula were found to be active in the investment stage, consistent with the search for the best outcome. As for the feedback period, results showed activation of areas related to memory, emotion and cues processing and executive decision making, like different parts of the frontal cortex. Previous studies had already reported some of these areas, including the superior and middle frontal gyrus and orbitofrontal cortex for complex value processing and executive functions in decision making. Analyses to feedback considering previously formed expectations, revealed activation of reward circuitry areas (e.g. midbrain, basal ganglia, OFC, anterior cingulate gyrus) when feedback and expectations matched.

The first analysis focused on the first decision moment of the experiment – Expectation phase. In this instant, participants were asked to estimate how much they were expecting to receive in the end of that negotiation round, in order to assess the neural mechanisms involved in the expectations of reward or punishment. So, participants had to look at the photo of the trustee that appeared on the screen and estimate how much they thought they would receive, according to a future investment made (possibly recalling previous interactions with him/her).

Interestingly, in the economic task, when they were expecting to receive low amounts of money (contrast High Expectation>Low Expectation), the postcentral gyrus showed higher activation than when they were expecting to receive higher amounts. This is odd because, in spite of being associated with choice selection [76], the postcentral gyrus had been associated with reward anticipation [77][78]. So, it would be expectable to have greater activation of this region when a high reward is expected. Contrarily, high expectations, revealed activation of the right cuneus, lingual gyrus and the superior parietal lobule comparing to low expectations. The cuneus and lingual gyrus are part of the occipital lobe and they have a role in visuospatial processing [79]. Both these visual regions plus motor cortex activations demonstrate engagement and concentration in the task presented. However, activation of these somatosensory cortex areas might only be due to the button pressing action. Though, since these regions should be active for both high and low expectations, this contrast should cancel their

activation. Yet, visual and motor regions seem more engaged when the participants have higher expectations. Additionally, the lingual gyrus has been stated as a fundamental structure in the attribution of intentions to others[80], which is consistent with this period of the experience. The superior parietal lobule has been shown to be crucial, not only in the visuospatial processes, but also in more cognitive operations such as manipulation of information in working memory, together with dorsolateral prefrontal cortex [81]. This is a role which is central to the prefrontal cortex, but frontoparietal connections are relevant in this context. To build expectations, participants have to recall previous interactions. Parietal cortex seems to be highly activated in an expectation and reward anticipation scenario that shows considerable activation. It would be predictable that areas associated with learning, reward anticipation, differential choice and even memory would be active, such as the anterior cingulate gyrus, the middle frontal gyrus and the precentral gyrus [81]. The fact that these areas do not exhibit activation in this contrast is probably due to the fact that they are active with both high and low expectations and, therefore, cancel themselves. Hemispheric patterns were also observed, some of which expected from the type of response output. As explained, subjects had the three button-response box on top of them. To select high values, they had to press the right button and to select low values, the left button. It is, thus, interesting to note that sensorimotor responses related to high expectations come associated with the left hemisphere and low expectations with activations of the right hemisphere.

The same contrast was performed (High Expectation>Low Expectation), for the exact same moment in the health-related task, but, in this case the results were quite different. Activations in the middle temporal gyrus (MTG), GP, midbrain and midcingulate gyrus (MCG) were particularly relevant due to their involvement in perceptual and learning processes and emotional judgment [82][83]. The MTG and the anterior cingulate gyrus have been postulated to be active in the complex process of attributing intentions to others [80] and conflict monitoring (ACC), which is consistent with this phase of the experience, since participants had to look to the photo of the trustee and try to perceive his/her intentions. The GP, for instance, as a subcortical structure, part of the basal ganglia, is associated with perceptual decision making [84]. More specifically, the GP, as well as the caudate, have been claimed to have an important role in detecting others behavior and might be involved in goal-oriented behavior [85]. The activity of the midbrain dopaminergic neurons has been reported to

be involved in decision making, particularly in risky decision making [86][87]. Also, this activity has been said to increase with gains [88] which is consistent with the results showing increased differential activation for high expectations. This area seems to have a role in the calculation of future outcomes and thus perhaps comprises a neural feedback loop regarding risk-reward decision making. The MCG has also been implicated in deductive reasoning [89], memory [81] and attention [90] processes. Activation of these regions seems to emphasize their role in the evaluation of others (mentalizing) and also in remembering previous interactions to adjust their decisions. The lingual gyrus was also found to be one of the structures involved in the process of attributing intentions to others [80]. Though, contrarily to the middle temporal gyrus, it showed more activation when people expected to wait more time (Lower Expectations) compared to when they expected to wait less (higher expectations). The expectation period seems to be an evaluation period, where participants infer others behavior or traits in order to create predictions for a future outcome. This input given by the participant also allows us to later confirm whether the outcome was higher or lower than what he/she was expecting.

Regarding the investment period, in both tasks (Economic and Health related), there was a differential activation in the precentral gyrus, when performing the contrast High Investment>Low Investment. The precentral gyrus participates in the cognitive control [91] and is involved in the mirror neuron system [92]. This system is responsible for mimicking actions that we perceive as good and, thus, allows us to better understand others behavior. However, comes more often associated with mimicking movements and our game only shows pictures. As stated before, the somatosensory cortex activation might have a simpler explanation related to the button pressing demanded by the task. Nevertheless, the precentral gyrus is recognized as one of the areas activated in uncertain reward-based contexts [88]. Low investments in the economic task also showed increased activation, compared to high investments, in the insula and posterior cingulate gyrus (PCG). The insular cortex activation is one of the major results of these analyses, since is an area reported in different phases of the decision making process [14][93] and implicated in studies of reward learning as part of a neural circuit that guides and adjusts behavior on the basis of reward feedback [14]. The PCG area, besides being associated with mentalizing (theory of mind), as stated in the Overwalle et al. 2009 review [29], it is also related to action selection with expectation for large reward values [94][95], contrarily to what functional results show. Moreover, the PCG

is a part of a brain circuit that processes inputs from the limbic system and it is related to evaluative functions that lead to response generation [94]. This is consistent with the functional results obtained, since it has been reported that emotions play an important role in decision making [26].

The last phase of each decision making round comes with the feedback to the participants' actions. Here, activation of the prefrontal cortex (BA 6 and 10) is the most notable finding for both economic and health-related decision making. MTG (BA19) activation was also seen in the economic-related decision making. All of these brain regions showed increased activation when participants received a high reward. Activation of the frontal cortex, particularly the OFC region, was expected given the notion that the corticostriatal circuitry is involved in reward and emotion in decision making [96] [97] as well as complex processing of indicators that guide decision making [77] [98]. The MTG has been reported to be active during the reward process as well [96] and also in perception of others' intentions [99][100][101]. The active areas, besides being involved in reward anticipation [77][102], are, more importantly, involved in deductive and inferential reasoning [89][103] and processing self and others emotions [101][104]. The fact that areas related to perception of others [80][100] were active, suggests that participants were already updating information regarding that trustee and thinking about the next iteration.

When expectations did not match the outcome values (contrast High Reward Low Expectation > Low Reward High Expectation), there was an increased activation in perception areas (e.g. fusiform gyrus) [100] in the economic-related decision making. Receiving greater amounts than expected activated the fusiform gyrus and right lingual gyrus. All of these areas have been reported to be involved in face recognition and perceiving of others [100].

For a more thorough examination, and given that relative reward vs punishment are not symmetrical, contrasts of these unmatched expectations were compared to the baseline. When the feedback was higher than expected in the economic-related task, there was significant activation of prefrontal areas, such as the middle frontal gyrus, thus, indicating an emotional processing and planning of future actions [105]. Activation of the anterior insula and precentral gyrus was also noted. These areas are involved in emotional processing and reasoning as well as perceiving and attribution of intentions to others. The activation of reward circuits is consistent with a greater gain

than expected and the prefrontal cortex and precentral gyrus activation suggests that participants were already planning their next action based on this new information. Similarly, the health-related task results also showed greater activation of the prefrontal cortex and "mirror neuron system" when the reward was higher than expected.

When participants received less than they expected ("Punishment") in the economic-related task, activation of the prefrontal cortex, precentral gyrus and anterior insula was observed, like when the reward was higher than expected. This corroborates the suggestion that participants analyze the feedback and update information regarding that trustee, and immediately start planning their next action. However, it was interesting to observe that in both health and economic related tasks, there was a deactivation of the caudate region. This suggests that the caudate is more associated with learning of positive reward values. Though, this might mean that the role of this structure in the adjustment of information given the feedback obtained have distinct weight during losses as compared to gain. In the health-related task, once again, like when feedback was higher than expected, prefrontal areas activated.

For outcomes fitting the previously formed expectations, areas such as superior and middle frontal gyrus, anterior cingulate gyrus, orbitofrontal cortex and anterior insula were found to be active for high expectations and high feedback values. The middle frontal gyrus has already been said to have a role in emotional processing and planning of future actions [105]. This activation is particularly important since feedback results for this contrast matched the expectations, which suggests an understanding and prediction of the trustee's behavior. Anterior insula is also related to emotion processing and consciousness [3][21][106] and consequently involved in the prediction process and consequent reward processing. The gyrus rectus is also a key region since, as part of the OFC, is active in decision making involving reward [107][77] and reward learning as it stores a certain stimulus as reward stimuli [108]. The OFC has a central role in the limbic system and emotional control. Therefore, its activation is extremely relevant in a reward based decision making context. All this structures take part in the reward pathway and, consequently, in the emotional judgment [83], learning and decision processes associated. These results show a complete involvement of subcortical regions, especially in the health-related decision making and suggest an important role of these structures in the expectations period, particularly in high expectations and high rewards trials.

5.2 Conclusion

This project aimed to identify the cerebral regions involved in the different moments of high-level decision making scenarios, economical and health related and to identify the role of cortical and subcortical regions.

Although many studies and research projects have focused on brain regions activations' in a decision making context, the use of self-relevant health related variables represent a novel approach in this field. In this project, contrast analyses parsing distinct cognitive components of the decision making process were performed showing differential activation of some relevant brain areas. The experimental paradigm designed was then, according to the results, validated and allowed to evaluate the neural correlates of decision making in different contexts.

Results show that the decision making process is flexible and depends not only on the outcomes and interactions for modulating different brain responses, but it also depends on the context. In the economic related decision making, there was preferential activation of the prefrontal and perceptive areas.

However, in the health related decision making more areas associated with emotional processing were active. This suggests that the economic topic, although being important to individuals, has an extrinsic value to the person and requires more rational and executive functions. The health context, for instance, has a more intrinsic value and appeals to the emotional side of individuals.

All things considered, these results show differential involvement of structures reported as core regions in decision making, thus, validating the experimental paradigm. The differential activation of midbrain, OFC and insula are the most prominent findings, as these areas are central regions of emotional control and processing, thus, showing a key involvement of the limbic system in a risk-reward decision making context.

Chapter 6

Limitations and Future work

The purpose/objective of this project was to clarify the brain regions involved in high-level decision making contexts and this was accomplished with relative success.

The fact that both tasks were conducted one after another without intermission does not permit direct comparison and the economic task mainly attempts to replicate previous experiments. Performing each task procedure (economic and clinical) separately could be considered, in the future, in a random balanced way.

Importantly, a different game structure could be considered. Although results were noteworthy, the game design could be more captivating and stimulating. The participants' learning process would be better evaluated if iterations were continuous or, at least, co-dependent with each trustee (which is what happens in real life and would create randomization/balance difficulties). Besides, having a more challenging task (e.g. including rewards, marks or achievements) would probably engage participants a bit more.

Nonetheless, in order to obtain more robust data, the number of participants should be higher (although we still had enough statistical power for random effects analyses). Behavioral data gathering prior the tasks should also be considered, such as personality test and risk profile evaluations (this was actually done beyond the scope of this project). With a higher number of subjects and behavioral data tests, different group analyses can be considered - participants could be stratified considering, for example, their risk profile. Also, implementation of this paradigm in disease models and group comparisons ought to be performed, as it was defined as a mid-long term objective.

Analyses considering the interaction of the participant with each trustee must be of further consideration too. This may allow us to understand if decision making and risk taking options are only based upon previous social interaction experiences.

Finally, given that several brain structures have been reported to have a crucial role in decision making processes, social cognition and risk taking actions (e.g. Pre-frontal cortex [109], reward circuitry [16][14] and anterior cingulate gyrus [9], ROI analyses, namely in the nucleus accumbens and the amygdala, might be a pertinent and more focused approach. Furthermore, given the relatively short TR used (TR=2sec), connectivity analyses can probably be performed and might be the logical next step.

References

[1]   M. J. Frank and R. C. O'Reilly, "A Mechanistic Account of Striatal Dopamine Function in Human Cognition: Psychopharmacological Studies With Cabergoline and Haloperidol," *Behav. Neurosci.*, vol. 120, no. 3, pp. 497–517, 2006.

[2]   A. G. Sanfey, "Social Decision-Making: Insights from Game Theory and Neuroscience," *Science (80-.).*, vol. 318, pp. 881–883, 2007.

[3]   J. Decety, P. Jackson, J. Sommerville, and E. Al., "The neural bases of cooperation and competition: an fMRI investigation," *Neuroimage*, vol. 23, no. 2, pp. 744–751, 2004.

[4]   G. E. Bolton, E. Katok, and R. Zwick, "Dictator game giving: Rules of fairness versus acts of kindness," *Int. J. Game Theory*, vol. 27, no. 2, pp. 269–299, 1998.

[5]   J. R. Stevens and M. D. Hauser, "Why be nice? Psychological constraints on the evolution of cooperation," *Trends Cogn. Sci.*, vol. 8, no. 2, pp. 60–65, 2004.

[6]   J. H. Flavell, "COGNITIVE DEVELOPMENT : Children's Knowledge About the Mind," *Annu. Rev. Psychol*, vol. 50, pp. 21–45, 1999.

[7] G. Loewenstein, S. Rick, and J. D. Cohen, "Neuroeconomics," *Annu. Rev. Psychol.*, vol. 59, no. 1, pp. 647–672, 2008.

[8] S. B. R. E. Brown and K. R. Ridderinkhof, "Aging and the neuroeconomics of decision making: A review," *Cogn. Affect. Behav. Neurosci.*, vol. 9, no. 4, pp. 365–379, 2009.

[9] F. van Winden, M. Stallen, and R. Ridderinkhof, "On the Nature, Modeling, and Neural Bases of Social Ties," 2008.

[10] K. McCabe, D. Houser, L. Ryan, V. Smith, and T. Trouard, "A functional imaging study of cooperation in two-person reciprocal exchange," *Proc. Natl. Acad. Sci. U. S. A.*, vol. 98, no. 20, pp. 11832–11835, 2001.

[11] F. Krueger, K. McCabe, J. Moll, N. Kriegeskorte, R. Zahn, M. Strenziok, A. Heinecke, and J. Grafman, "Neural correlates of trust.," *Proc. Natl. Acad. Sci. U. S. A.*, vol. 104, no. 50, pp. 20084–20089, 2007.

[12] B. King-Casas, D. Tomlin, C. Anen, and E. Al., "Getting to Know You: Reputation and Trust in a Two-Person Economic Exchange," *Science (80-.).*, vol. 308, no. 5718, pp. 78–83, 2005.

[13] D. Tomlin, M. A. Kayali, B. King-Casas, C. Anen, C. F. Camerer, S. R. Quartz, and P. R. Montague, "Agent-Specific Responses in the Cingulate Cortex During Economic Exchanges.," *Science (80-.).*, vol. 312, no. 5776, pp. 1047–1050, 2006.

[14] M. R. Delgado, M. M. Miller, S. Inati, and E. A. Phelps, "An fMRI study of reward-related probability learning," *Neuroimage*, vol. 24, no. 3, pp. 862–873, 2005.

[15] J. K. Rilling, D. A. Gutman, T. R. Zeh, G. Pagnoni, G. S. Berns, and C. D. Kilts, "A Neural Basis for Social Cooperation," *Neuron*, vol. 35, no. 2, pp. 395–405, 2002.

[16] T. Singer, B. Seymour, J. P. O. Doherty, K. E. Stephan, R. J. Dolan, and C. D. Frith, "Empathic neural responses are modulated by the perceived fairness of others," *Nature*, vol. 439, no. 7075, pp. 466–469, 2006.

[17] R. Hardin, "Trustworthiness," *Ethics*, vol. 107, no. 1. pp. 26–42, 1996.

[18] E. M. Uslaner, "Trust and Corruption," 2004.

[19] G. I. Christopoulos, P. N. Tobler, P. Bossaerts, R. J. Dolan, and W. Schultz, "Neural Correlates of Value, Risk, and Risk Aversion Contributing to Decision Making under Risk," *J. Neurosci.*, vol. 29, no. 40, pp. 12574–12583, 2009.

[20] J. K. Rilling and A. G. Sanfey, "The Neuroscience of Social Decision Making," *Annu. Rev. Psychol.*, vol. 62, pp. 23–48, 2011.

[21] K. M. Harlé and A. G. Sanfey, "Social economic decision-making across the lifespan: an fMRI investigation," *Neuropsychologia*, vol. 50, no. 7, pp. 1416–1424, 2012.

[22] D. Dunning, J. E. Anderson, T. Schlösser, D. Ehlebracht, and D. Fetchenhauer, "Trust at Zero Acquaintance: More a Matter of Respect Than Expectation of Reward.," *J. Pers. Soc. Psychol.*, vol. 107, no. 1, pp. 122–41, 2014.

[23] A. K. J. Fett, P. M. Gromann, V. Giampietro, S. S. Shergill, and L. Krabbendam, "Default distrust? An fMRI investigation of the neural development of trust and cooperation," *Soc. Cogn. Affect. Neurosci.*, vol. 9, no. 4, pp. 395–402, 2014.

[24] E. Fouragnan, G. Chierchia, S. Greiner, R. Neveu, P. Avesani, and G. Coricelli, "Reputational Priors Magnify Striatal Responses to Violations of Trust.," *J. Neurosci.*, vol. 33, no. 8, pp. 3602–3611, 2013.

[25] J. Berg, J. Dickhaut, and K. McCabe, "Trust, Reciprocity, and Social History," *Games Econ. Behav.*, vol. 10, no. 1, pp. 122–142, 1995.

[26] A. G. Sanfey, J. K. Rilling, J. A. Aronson, L. E. Nystrom, and J. D. Cohen, "The Neural Basis of Economic Decision Making in the Ultimatum Game," *Science (80-.).*, vol. 300, pp. 1755–1758, 2003.

[27] L. J. Chang, A. Smith, M. Dufwenberg, and A. G. Sanfey, "Triangulating the Neural, Psychological, and Economic Bases of Guilt Aversion," *Neuron*, vol. 70, no. 3, pp. 560–572, 2011.

[28] W. van den bos, E. van Dijk, M. Westenberg, S. A. R. B. Rombouts, and E. A. Crone, "What motivates repayment? Neural correlates of reciprocity in the Trust Game," *Soc. Cogn. Affect. Neurosci.*, vol. 4, no. 3, pp. 294–304, 2009.

[29] F. Van Overwalle and K. Baetens, "Understanding others' actions and goals by mirror and mentalizing systems: A meta-analysis," *Neuroimage*, vol. 48, no. 3, pp. 564–584, 2009.

[30] S. Sheth, M. Mian, S. Patel, and E. Al., "Human Dorsal Anterior Cingulate Cortex Neurons Mediate Ongoing Behavioral Adaptation," *Nature*, vol. 488, no. 7410, pp. 218–221, 2012.

[31] S. A. Huettel, A. W. Song, and G. McCarthy, *Functional Magnetic Resonance Imaging*, vol. 67. 2008.

[32] V. Van Veen, C. B. Holroyd, J. D. Cohen, V. A. Stenger, and C. S. Carter,

"Errors without conflict: Implications for performance monitoring theories of anterior cingulate cortex," *Brain Cogn.*, vol. 56, no. 2 SPEC. ISS., pp. 267–276, 2004.

[33] Y. Wang, Z. Zhang, Y. Jing, E. A. Valadez, and R. F. Simons, "How Do We Trust Strangers? The Neural Correlates of Decision Making and Outcome Evaluation of Generalized Trust," *Soc. Cogn. Affect. Neurosci.*, 2016.

[34] G. Dong, X. Lin, H. Zhou, and Q. Lu, "How the win-lose balance situation affects subsequent decision-making: Functional magnetic resonance imaging evidence from a gambling task," *Neuroscience*, vol. 272, pp. 131–140, 2014.

[35] G. Xue, Z. Lu, I. P. Levin, and A. Bechara, "An fMRI study of Risk-Taking Following Wins and Losses: Implications for the Gambler's Fallacy?," *Hum. Brain Mapp.*, vol. 32, no. 2, pp. 271–281, 2011.

[36] U. Schmidt and H. Zank, "A simple model of cumulative prospect theory," *J. Math. Econ.*, vol. 45, no. 3–4, pp. 308–319, 2009.

[37] S. H. Mitchell and V. B. Wilson, "The subjective value of delayed and probabilistic outcomes: Outcome size matters for gains but not for losses," *Behav Process.*, vol. 83, no. 1, p. 36, 2010.

[38] M. Brand, K. Labudda, E. Kalbe, and E. Al., "Decision-making impairments in patients with Parkinson's disease," *Behav. Neurol.*, vol. 15, pp. 77–85, 2004.

[39] N. R. Glassman, "Magnetic Resonance Imaging," *J. Consum. Health Internet*, vol. 14, no. 3, pp. 308–321, 2010.

[40] D. Linden, "Neurofeedback and networks of depression," *Dialogues Clin. Neurosci.*, vol. 16, no. 1, pp. 103–112, 2014.

[41] M. J. Sands and A. Levitin, "Basics of Magnetic Resonance Imaging," *Semin. Vasc. Surg.*, vol. 17, no. 2, pp. 66–82, 2004.

[42] J. P. Hornak and D. Ph, "The Basics of MRI," 1997. [Online]. Available: http://www.cis.rit.edu/htbooks/mri/index.html. [Accessed: 10-Aug-2016].

[43] J. M. T. dos Anjos, "Nuclear Magnetic Resonance." [Online]. Available: http://fisica-microfisica.blogspot.pt/2013/10/medicina-nuclear.html. [Accessed: 10-Aug-2016].

[44] I. R. Violante, "The neurobiological basis of Neurofibromatosis type I: new insights into brain structure, function and neurochemistry," pp. 1–191, 2012.

[45] R. Goebel, "Localization of Brain Activity using Functional Magnetic Resonance Imaging," *Clin. Funct. MRI*, pp. 9–51, 2007.

[46] J. P. Ridgway, "Cardiovascular magnetic resonance physics for clinicians: part I," *J. Cardiovasc. Magn. Reson.*, vol. 12, no. 1, p. 71, 2010.

[47] C. J. Aine, "A Conceptual Overview and Critique of Functional Neuroimaging Techniques in Humans: I.MRI/fMRI and PET," *Crit. Rev. Neurobiol.*, vol. 9, pp. 229–309, 1995.

[48] "MRI-Image density and contrast." [Online]. Available: http://mri-2010.blogspot.pt/2010/10/october-lecture-notes-1-image-density.html. [Accessed: 20-Aug-2016].

[49] A. D. Elster, "Questions and Answers in MRI - Image Contrast." [Online]. Available: http://mriquestions.com/image-contrast-trte.html. [Accessed: 10-Aug-2016].

[50] S. Ogawa, T. M. Lee, A. R. Kay, and D. W. Tank, "Brain magnetic resonance imaging with contrast dependent on blood oxygenation.," *Proc. Natl. Acad. Sci. U. S. A.*, vol. 87, no. 24, pp. 9868–9872, 1990.

[51] S. Ogawa, D. W. Tank, R. Menon, J. M. Ellermann, S. G. Kim, H. Merkle, and K. Ugurbil, "Intrinsic signal changes accompanying sensory stimulation: Functional brain mapping with magnetic resonance imaging," *Proc. Natl. Acad. Sci. U. S. A.*, vol. 89, no. 13, pp. 5951–5955, 1992.

[52] K. K. Kwong, J. W. Belliveau, D. A. Chesler, I. E. Goldberg, R. M. Weisskoff, B. P. Poncelet, D. N. Kennedy, B. E. Hoppel, M. S. Cohen, and R. Turner, "Dynamic magnetic resonance imaging of human brain activity during primary sensory stimulation.," *Proc. Natl. Acad. Sci. U. S. A.*, vol. 89, no. 12, pp. 5675–5679, 1992.

[53] T. Christen, D. S. Bolar, and G. Zaharchuk, "Imaging Brain Oxygenation with MRI Using Blood Oxygenation Approaches: Methods, Validation, and Clinical Applications," *AJNR. Am. J. Neuroradiol.*, vol. 34, pp. 1113–23, 2013.

[54] M. M. Monti, "Statistical analysis of fMRI time-series: a critical review of the GLM approach," *Front. Hum. Neurosci.*, vol. 5, no. 609, p. 28, 2011.

[55] "BrainVoyager Support." [Online]. Available: http://support.brainvoyager.com/. [Accessed: 18-Aug-2016].

[56] S. Kiebel and A. Holmes, *The general linear model*. 2003.

[57] J. B. Poline and M. Brett, "The general linear model and fMRI: Does love last forever?," *Neuroimage*, vol. 62, no. 2, pp. 871–880, 2012.

[58] K. J. Friston, A. P. Holmes, K. J. Worsley, J.-P. Poline, C. D. Frith, and R. S. J.

Frackowiak, "Statistical Parametric Maps in Functional Imaging: A General Linear Approach," *Hum. Brain Mapp.*, vol. 2, no. 4, pp. 189–210, 1995.

[59] K. Worsley, C. Liao, J. Aston, V. Petre, G. Duncan, F. Morales, and A. Evans, "A General Statistical Analysis for fMRI Data," *Neuroimage*, vol. 15, pp. 1–15, 2002.

[60] A. P. Holmes and K. J. Friston, "Generalisability, Random Effects and Population Inference," *Neuroimage*, vol. 7, p. S754, 1998.

[61] R. Sladky, K. J. Friston, J. Trostl, R. Cunnington, E. Moser, and C. Windischberger, "Slice-timing effects and their correction in functional MRI," *Neuroimage*, vol. 58, no. 2, pp. 588–594, 2011.

[62] S. S. Statistics, M. F. Analysis, and A. F. Analysis, "FMRI Pre-Processing and Model- Based Statistics FMRI Pre-Statistics."

[63] K. J. Friston, O. Josephs, E. Zarahn, A. P. Holmes, S. Rouquette, and J.-B. Poline, "To Smooth or Not to Smooth?," *Neuroimage*, vol. 12, no. 2, pp. 196–208, 2000.

[64] K. J. Worsley and K. J. Friston, "Analysis of fMRI Time-Series Revisited - Again," *Neuroimage*, vol. 2, pp. 173–181, 1995.

[65] K. J. Friston, a P. Holmes, C. J. Price, C. Büchel, and K. J. Worsley, "Multisubject fMRI Studies and Conjunction Analyses.," *Neuroimage*, vol. 10, no. 4, pp. 385–396, 1999.

[66] J. Culham, "fMRI Data Quality Assurance and Preprocessing." [Online]. Available: http://slideplayer.com/slide/4831450/. [Accessed: 15-Aug-2016].

[67] S. M. Rajtmajer, A. Roy, R. Albert, P. C. M. Molenaar, and F. G. Hillary, "A voxelwise approach to determine consensus regions-of-interest for the study of brain network plasticity.," *Front. Neuroanat.*, vol. 9, p. 97, 2015.

[68] F. Godenschweger, U. Kägebein, D. Stucht, U. Yarach, A. Sciarra, R. Yakupov, F. Lüsebrink, P. Schulze, and O. Speck, "Motion correction in MRI of the brain.," *Phys. Med. Biol.*, vol. 61, no. 5, pp. R32–R56, 2016.

[69] T. R. Oakes, T. Johnstone, K. S. Ores Walsh, L. L. Greischar, A. L. Alexander, A. S. Fox, and R. J. Davidson, "Comparison of fMRI motion correction software tools," *Neuroimage*, vol. 28, no. 3, pp. 529–543, 2005.

[70] J. B. Hopfinger, C. Buchel, A. P. Holmes, and K. J. Friston, "A study of analysis parameters that influence the sensitivity of event-related fMRI analyses," *Neuroimage*, vol. 11, no. 4, pp. 326–333, 2000.

[71] M. Sacchet and B. Knutson, "Spatial smoothing systematically biases the localization of reward-related brain activity," *Neuroimage*, vol. 4, no. 164, pp. 270–277, 2013.

[72] P. M. Matthews and P. Jezzard, "Functional magnetic resonance imaging.," *J. Neurol. Neurosurg. Psychiatry*, vol. 75, no. 1, pp. 6–12, 2004.

[73] E. Amaro and G. J. Barker, "Study design in fMRI: Basic principles," *Brain Cogn.*, vol. 60, no. 3, pp. 220–232, 2006.

[74] "fMRI : block design paradigm." [Online]. Available: http://radiopaedia.org/images/626891. [Accessed: 18-Aug-2016].

[75] M. Osman, "The role of reward in dynamic decision making," *Front. Neurosci.*, vol. 6, p. 35, 2012.

[76] M. A. Addicott, D. A. A. Baranger, R. V. Kozink, M. J. Smoski, G. S. Dichter, and F. J. McClernon, "Smoking withdrawal is associated with increases in brain activation during decision making and reward anticipation: A preliminary study," *Psychopharmacology (Berl).*, vol. 219, no. 2, pp. 563–573, 2012.

[77] M. Ernst, E. E. Nelson, E. B. McClure, C. S. Monk, S. Munson, N. Eshel, E. Zarahn, E. Leibenluft, A. Zametkin, K. Towbin, J. Blair, D. Charney, and D. S. Pine, "Choice selection and reward anticipation: an fMRI study," *Neuropsychologia*, vol. 42, no. 12, pp. 1585–1597, 2004.

[78] M. P. Paulus, J. S. Feinstein, D. Leland, and A. N. Simmons, "Superior temporal gyrus and insula provide response and outcome-dependent information during assessment and action selection in a decision-making situation," *Neuroimage*, vol. 25, no. 2, pp. 607–615, 2005.

[79] R. Cabeza, F. Dolcos, S. E. Prince, H. J. Rice, D. H. Weissman, and L. Nyberg, "Attention-related activity during episodic memory retrieval: a cross- function fMRI study," *Neuropsychologia*, vol. 41, pp. 390–399, 2003.

[80] E. Brunet, Y. Sarfati, M. C. Hardy-Baylé, and J. Decety, "A PET Investigation of the Attribution of Intentions with a Nonverbal Task," *Neuroimage*, vol. 11, no. 2, pp. 157–166, 2000.

[81] J. X. Zhang, H. C. Leung, and M. K. Johnson, "Frontal activations associated with accessing and evaluating information in working memory: An fMRI study," *Neuroimage*, vol. 20, no. 3, pp. 1531–1539, 2003.

[82] R. Elliott, J. L. Newman, O. a Longe, and J. F. W. Deakin, "Differential response patterns in the striatum and orbitofrontal cortex to financial reward in humans: a

parametric functional magnetic resonance imaging study.," *J. Neurosci.*, vol. 23, no. 1, pp. 303–307, 2003.

[83] L. Ding and J. Gold, "The basal ganglia's contributions to perceptual decision-making," *Neuron*, vol. 79, no. 4, pp. 640–649, 2013.

[84] W. Wei, J. E. Rubin, X.-J. X. Wang, X. J. E. Rubin, and X.-J. X. Wang, "Role of the Indirect Pathway of the Basal Ganglia in Perceptual Decision Making," *J. Neurosci.*, vol. 35, no. 9, pp. 4052–4064, 2015.

[85] N. Arimura, Y. Nakayama, T. Yamagata, J. Tanji, and E. Hoshi, "Involvement of the globus pallidus in behavioral goal determination and action specification.," *J. Neurosci.*, vol. 33, no. 34, pp. 13639–53, 2013.

[86] G. Felsen and Z. F. Mainen, "Midbrain contributions to sensorimotor decision making," *J. Neurophysiol.*, vol. 108, no. 1, pp. 135–147, 2012.

[87] A. G. Sanfey, G. Loewenstein, S. M. McClure, and J. D. Cohen, "Neuroeconomics: cross-currents in research on decision-making," *Trends Cogn. Sci.*, vol. 10, no. 3, pp. 108–116, 2006.

[88] G. Z. Guo Z, Chen J, Liu S, Li Y, Sun B, "Brain areas activated by uncertain reward-based decision-making in healthy volunteers.," *Neural Regen. Res.*, vol. 8, no. 35, pp. 3344–3352, 2013.

[89] M. Knauff, T. Mulack, J. Kassubek, H. R. Salih, and M. W. Greenlee, "Spatial imagery in deductive reasoning: a functional MRI study," *Cogn. Brain Res.*, vol. 13, no. 2, pp. 203–212, 2002.

[90] C. S. Carter, M. Mintun, and J. D. Cohen, "Interference and Facilitation Effects during Selective Attention: an H215O PET study of Stroop Task Performance," *NeuroImage*, vol. 2, no. 4. pp. 264–272, 1995.

[91] J. Gläscher, R. Adolphs, H. Damasio, A. Bechara, D. Rudrauf, M. Calamia, L. K. Paul, and D. Tranel, "Lesion mapping of cognitive control and value-based decision making in the prefrontal cortex.," *Proc. Natl. Acad. Sci. U. S. A.*, vol. 109, no. 36, pp. 14681–14686, 2012.

[92] C. I. Hooker, K. A. Paller, D. R. Gitelman, T. B. Parrish, M. M. Mesulam, and P. J. Reber, "Brain Networks for Analyzing Eye Gaze," *Cogn. Brain Res.*, vol. 17, no. 2, pp. 406–418, 2003.

[93] J. Rebola, J. Castelhano, C. Ferreira, and M. Castelo-Branco, "Functional parcellation of the operculo-insular cortex in perceptual decision making: An fMRI study," *Neuropsychologia*, vol. 50, no. 14, pp. 3693–3701, 2012.

[94] A. N. McCoy, J. C. Crowley, G. Haghighian, H. L. Dean, and M. L. Platt, "Saccade Reward Signals in Posterior Cingulate Cortex," *Neuron*, vol. 40, no. 5, pp. 1031–1040, 2003.

[95] M. Wittmann, D. S. Leland, and M. P. Paulus, "Time and decision making: differential contribution of the posterior insular cortex and the striatum during a delay discounting task," *Exp. Brain Res.*, vol. 179, no. 4, pp. 643–653, 2007.

[96] X. Liu, J. Hairston, M. Schrier, and J. Fan, "Common and distinct networks underlying reward valence and processing stages: A meta-analysis of functional neuroimaging studies," *Neurosci. Biobehav. Rev.*, vol. 35, no. 5, pp. 1219–1236, 2011.

[97] J. M. Fuster, "The Prefrontal Cortex - An Update: Time Is of the Essence," *Neuron*, vol. 30, no. 2, pp. 319–333, 2001.

[98] and I.-J. J. Hackjin Kim, Min-Jo Choi, "Lateral OFC Activity Predicts Decision Bias due to First Impressions during Ultimatum Games," *J. Cogn. Neurosci.*, vol. 24, no. 2, pp. 428–439.

[99] S. Doallo, J. E. Raymond, K. L. Shapiro, M. Kiss, M. Eimer, and A. C. Nobre, "Response inhibition results in the emotional devaluation of faces: neural correlates as revealed by fMRI," *Soc. Cogn. Affect. Neurosci.*, vol. 7, no. 6, pp. 649–659, 2012.

[100] B. Rossion, C. Schiltz, and M. Crommelinck, "The functionally defined right occipital and fusiform 'face areas' discriminate novel from visually familiar faces," *Neuroimage*, vol. 19, no. 3, pp. 877–883, 2003.

[101] A. Todorov and A. D. Engell, "The role of the amygdala in implicit evaluation of emotionally neutral faces," *Soc. Cogn. Affect. Neurosci.*, vol. 3, no. 4, pp. 303–312, 2008.

[102] G. S. Berns, S. M. McClure, G. Pagnoni, and P. R. Montague, "Predictability Modulates Human Brain Response to Reward," *J. Neurosci.*, vol. 21, no. 8, pp. 2793–2798, 2001.

[103] C. Reverberi, P. Cherubini, A. Rapisarda, E. Rigamonti, C. Caltagirone, R. S. J. Frackowiak, E. Macaluso, and E. Paulesu, "Neural basis of generation of conclusions in elementary deduction," *Neuroimage*, vol. 38, no. 4, pp. 752–762, 2007.

[104] M. Deppe, W. Schwindt, H. Kugel, and E. Al., "Nonlinear Responses Within the Medial Prefrontal Cortex Reveal When Specific Implicit Information Influences

Economic Decision Making," *J. Neuroimaging*, vol. 15, no. 2, pp. 171–182, 2005.

[105] J. M. Fincham, C. S. Carter, V. van Veen, V. A. Stenger, and J. R. Anderson, "Neural mechanisms of planning: A computational analysis using event-related fMRI.," *Proc. Natl. Acad. Sci. U. S. A.*, vol. 99, no. 5, pp. 3346–3351, 2002.

[106] R. L. Peterson, "The neuroscience of investing: fMRI of the reward system," *Brain Res. Bull.*, vol. 67, no. 5, pp. 391–397, 2005.

[107] R. D. Rogers, A. M. Owen, H. C. Middleton, E. J. Williams, J. D. Pickard, B. J. Sahakian, and T. W. Robbins, "Choosing between Small, Likely Rewards and Large, Unlikely Rewards Activates Inferior and Orbital Prefrontal Cortex," *J. Neurosci.*, vol. 19, no. 20, pp. 9029–9038, 1999.

[108] L. K. Fellows, "Advances in understanding ventromedial prefrontal function: The accountant joins the executive," *Neurology*, vol. 68, no. 13, pp. 991–995, 2007.

[109] D. Knoch, L. R. R. Gianotti, A. Pascual-Leone, V. Treyer, M. Regard, M. Hohmann, and P. Brugger, "Disruption of Right Prefrontal Cortex by Low-Frequency Repetitive Transcranial Magnetic Stimulation Induces Risk-Taking Behavior," *J. Neurosci.*, vol. 26, no. 24, pp. 6469–6472, 2006.